

To: NVE  
Attn.: Odd-Arne Jensen  
Copy to:  
Date: 2022-04-07  
Revision no./Rev.date: 0 /  
Document no.: 20200017-06-TN  
Project: AARN - Applied Avalanche Research in Norway  
Project manager: Christian Jaedicke  
Prepared by: Peter Gauer, Henrik Langeland, Sean Salazar and Krister Kristensen  
Reviewed by: Sean Salazar

## **WP 2 – Full-scale experiments at Ryggfonn Ryggfonn avalanche observations 2020/2021**

### **Contents**

<b>1</b>	<b>Introduction</b>	<b>2</b>
<b>2</b>	<b>Research goals</b>	<b>2</b>
<b>3</b>	<b>Methods</b>	<b>2</b>
<b>4</b>	<b>Results</b>	<b>6</b>
	4.1 Weather data at the Fonnbu station	6
	4.2 Observations at Ryggfonn	8
<b>5</b>	<b>Concluding remarks</b>	<b>46</b>
<b>6</b>	<b>References</b>	<b>47</b>

### **Review and reference page**

## 1 Introduction

NGI continues to operate the avalanche test site at Ryggfonn in Stryn municipality, Vestland county, western Norway (61.969°N, 7.275°E). In addition to the field work and data collection performed in the context of WP2 – *Avalanche dynamics* in AARN, necessary repairs and updating of the data acquisition system at the Ryggfonn avalanche test site were carried out under this task. Maintenance was carried out to ensure that the site was ready for the 2021/22 winter season.

## 2 Research goals

A main challenge for avalanche research is to obtain a comprehensive understanding of the different flow regimes (dense, fluidized, or suspension flow) and of the involved physical processes. To obtain the necessary understanding, a combination of different measurements and observations is desirable to gain a broad and consistent picture of the avalanche flow. The understanding of complexity and variety of avalanche motion requires a combination of small-scale experiments (detailed investigations, statistics), large-scale tests (detailed investigation), and field observations (diversity, statistics). Cross-comparison between different avalanche paths (test sites) is necessary to uncover scaling relations, i.e. to identify differences in avalanche behaviour arising from variations in total length or slope along avalanche paths. Field observations and full-scale tests under controlled conditions are therefore necessary for the aforementioned reasons and as a basis for statistical analysis.

## 3 Methods

NGI's full-scale avalanche test site at Ryggfonn, near Stryn, has been operational since the early 1980's (Gauer et al. 2010; Gauer & Kristensen, 2016, and references therein). The facilities at Ryggfonn consist of the main and secondary avalanche tracks with a vertical drop of 950 m, a catchment dam at the base, and several instrumentation installations for monitoring avalanche dynamics (as depicted in Figure 1, Figure 2, Figure 3, and Figure 4). The current facility is one of only two in the world of this scale, and the catchment dam is a unique feature making this location the only place in the world where the efficiency of avalanche mitigation can be studied in full-scale.

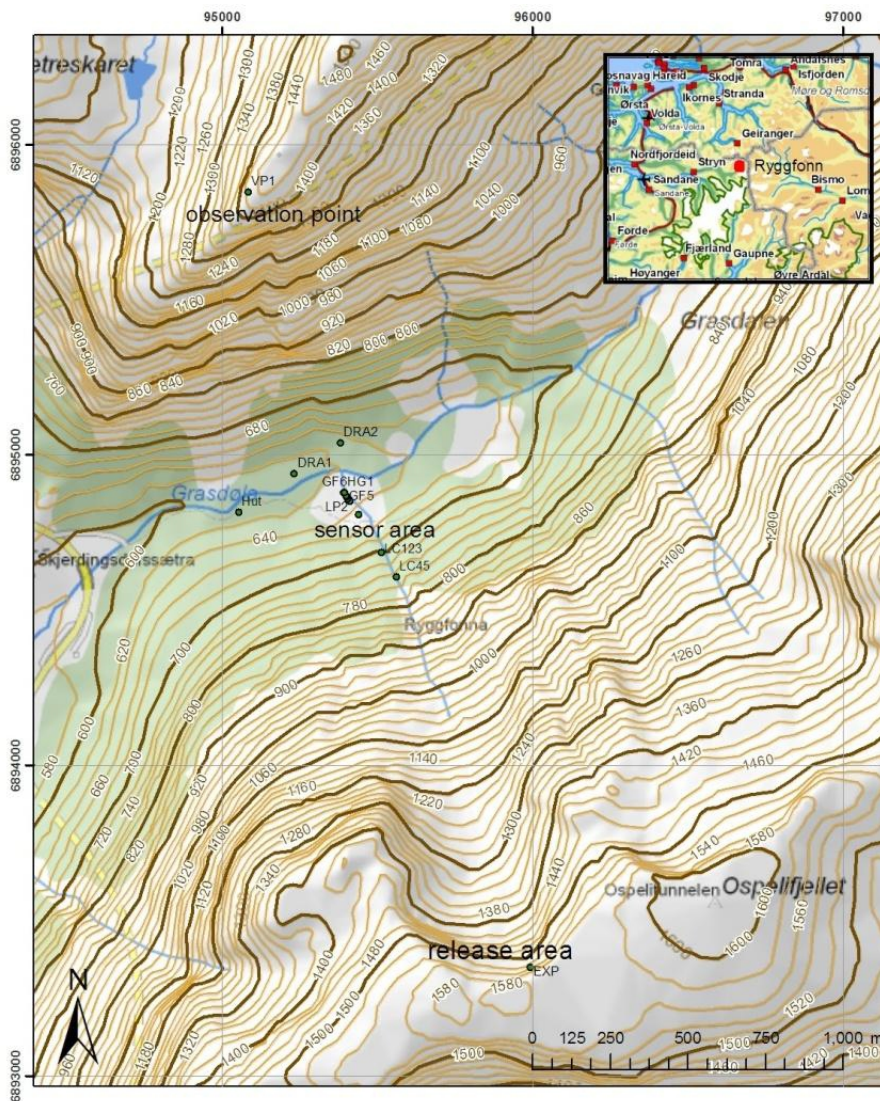


Figure 1 Map of the Ryggfonna test-site.

The NGI Ryggfonna facility was developed to obtain measurements to characterise avalanche dynamics and benchmark the development and calibration of numerical models. The full-scale testing facility is needed to investigate the complex dependency of avalanches on ambient conditions which cannot be reproduced in small-scale experiments. Data collected include velocity measurements, impact pressure measurements, and flow height measurements at selected locations along the avalanche track. Field investigations are performed to collect runout data and data on mass balance. Corresponding meteorological data are measured at a nearby NGI research station, Fonnbu.

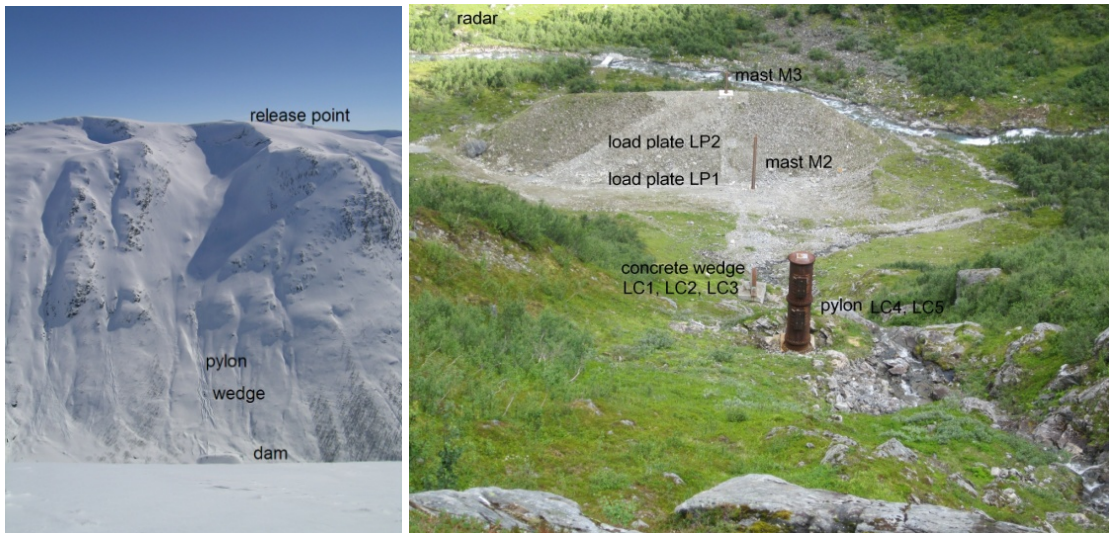


Figure 2 Existing NGI facility at Ryggfonn: (left) Avalanche track from the release area down to the retaining dam; (right) Example of sensor installations and full-scale pylon in the lower part of the avalanche track.

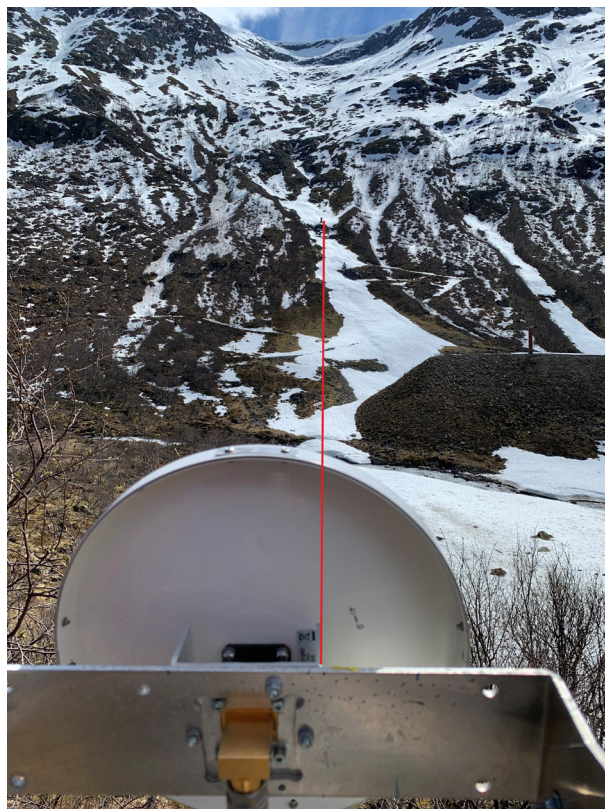


Figure 3 View from the radar position onto the track.

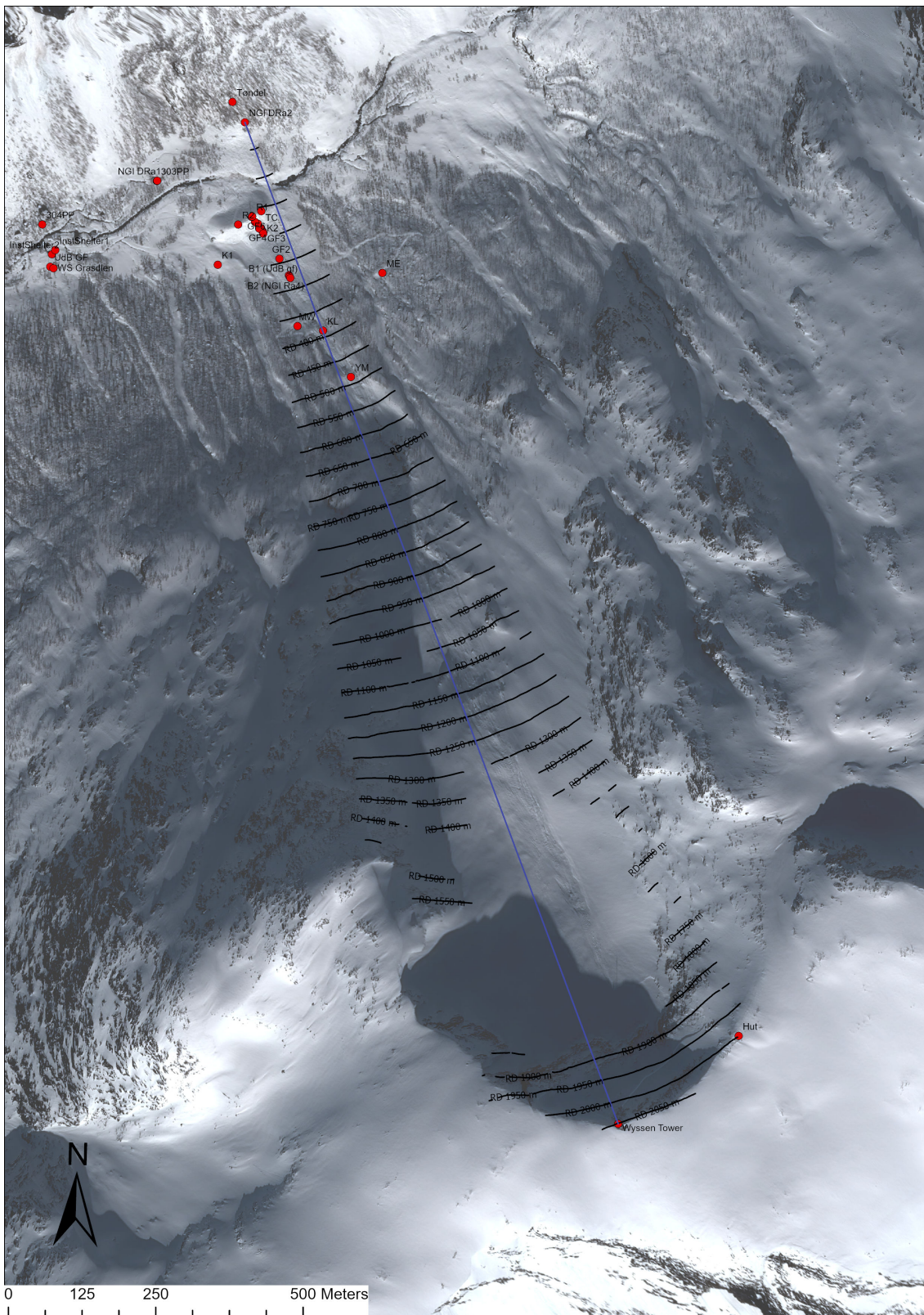


Figure 4 Radar field of view and radar range (50 m contour interval)

## 4 Results

Eight natural avalanches of size 2 to 3 (on the EAWS avalanche size scale) occurred during the winter 2020/2021. The avalanches released mid-February, during the second half of March, in the beginning of April, and early May. For some of the avalanche events, pressure data and/or rough estimates of local velocities, were collected. An autonomous Doppler radar system, installed in the fall of 2020, provided first velocity data for some of the events. Although field observations were carried out on few occasions after an event, the gained information was limited by weather constraints. In addition to measurements of natural releases, a field campaign was launched on 11.04.2021 resulting in a successful full-scale experiment. The released avalanche was of relative size R4 (EAWS size 4).

In Section 4.1 and Section 4.2, weather data and observation data are described, respectively. A brief overview of the collected data (sorted by date) and preliminary analyses are presented.

### 4.1 Weather data at the Fonnbu station

An overview of the major meteorological parameters monitored during the 2020/21 season is presented in Figure 5, Figure 6, and Figure 7.

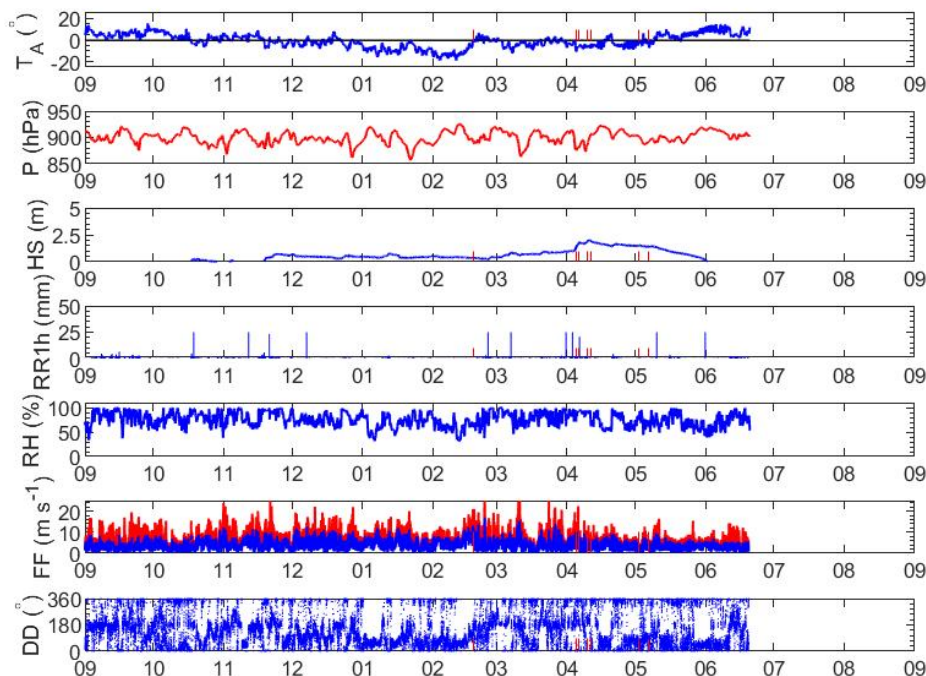


Figure 5 Fonnbu station: Overview of the major meteorological parameters (hourly data) during the season 2020/2021. The red stems in some of the plots indicate the date of the known avalanche event at Ryggfonn.

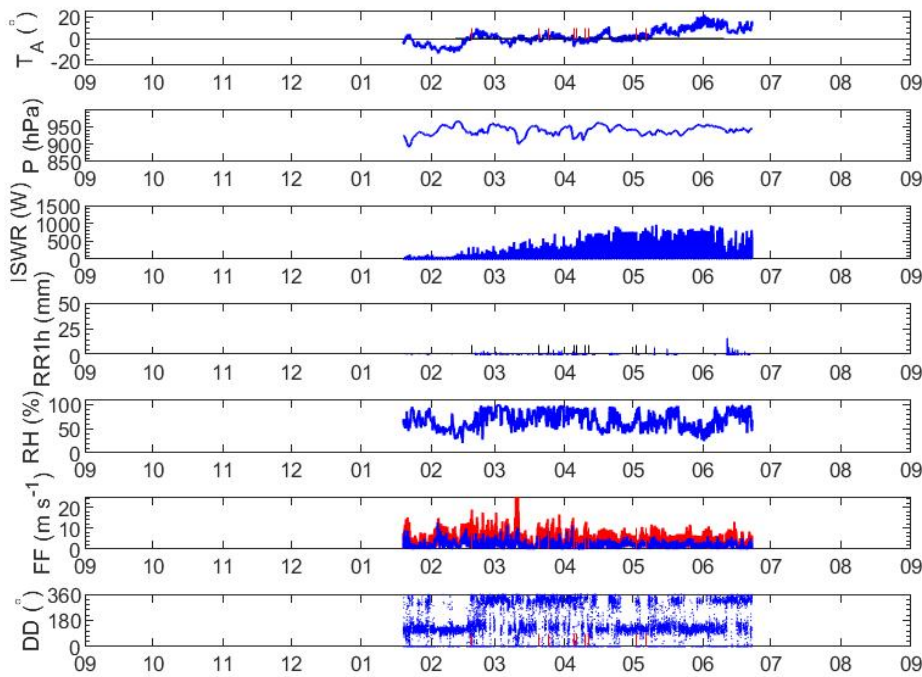


Figure 6 Grasdalen station: Overview of the major meteorological parameters during the season 2020/2021. The red stems in some of the plots indicate the date of the know avalanche event at Ryggfonn.

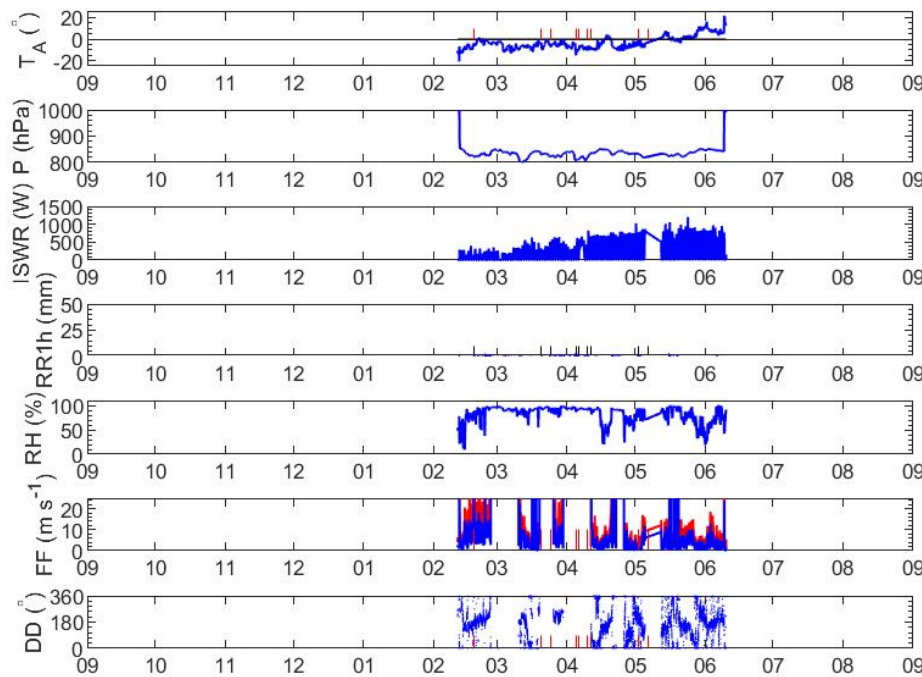


Figure 7 Ryggfonn station: Overview of the major meteorological parameters during the season 2020/2021. The red stems in some of the plots indicate the date of the know avalanche event at Ryggfonn.

## 4.2 Observations at Ryggfonn

### Velocity estimates

Table 1 Overview of natural avalanche release during 2020/2021;  $U_{LC}$  is the averaged velocity between the pylon and the concrete wedge;  $U_b$  the estimate velocity at the foot of the dam.

Date (yyyymmdd)	Time (CET)	$U_{LC}$ (m/s)	$U_b$ (m/s)
20210218	21:43	NaN	NaN
20200320	16:35	NaN	NaN
20200324	22:11	2 (uc)	NaN
20210405	07:01	37	28
20210406	06:04	28	22
20210410	01:54	NaN	NaN
20210411	15:08	43	41
20210502	12:56	NaN	NaN
20210506	16:49	NaN	NaN

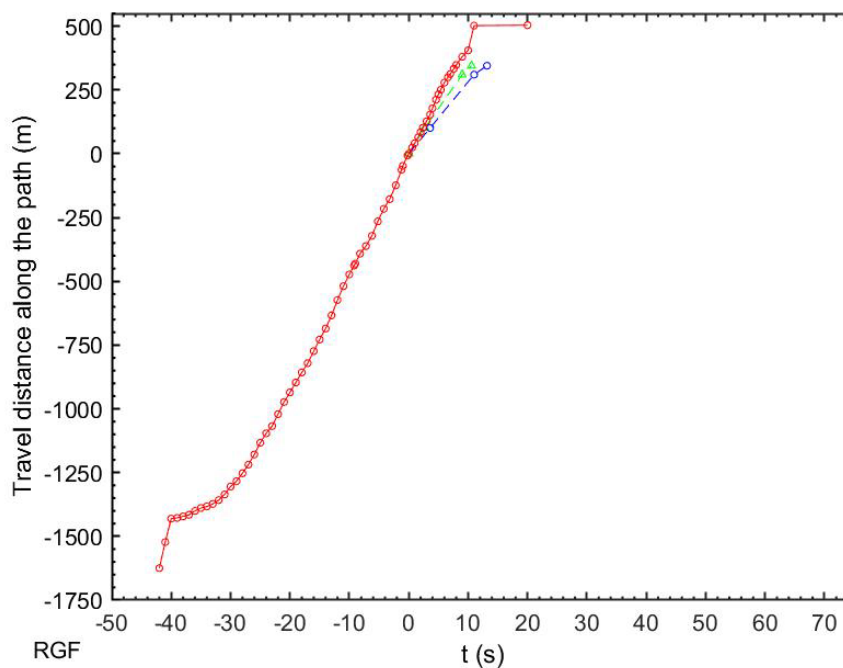


Figure 8 Timing of the avalanche.  $T=0$  at the pylon,  $T1$  at concrete wedge, and  $T2$  at Mast M2 (LC45, and LC123 in Figure 1 and Figure 2).



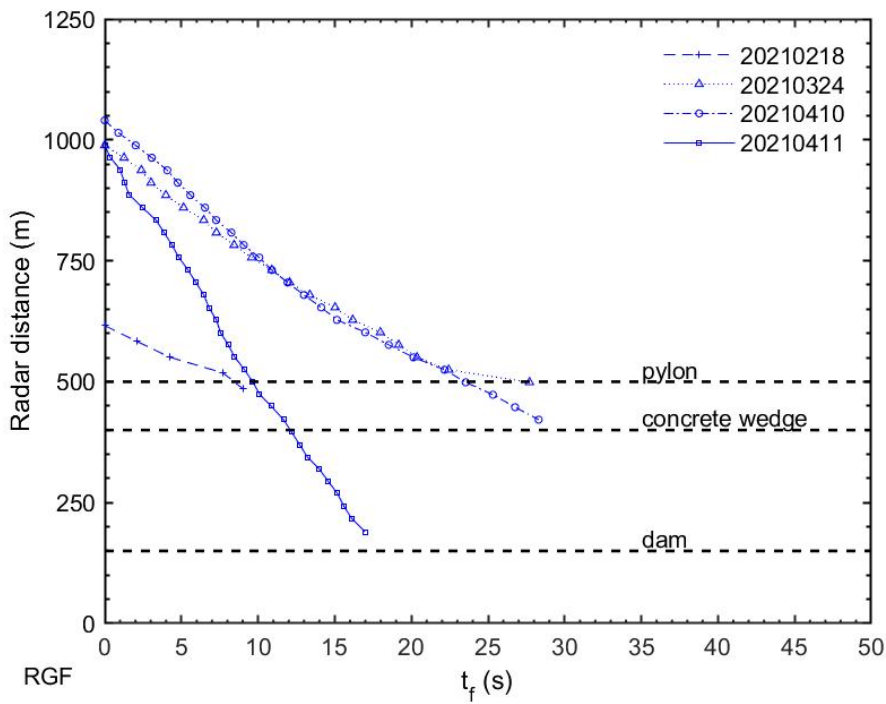
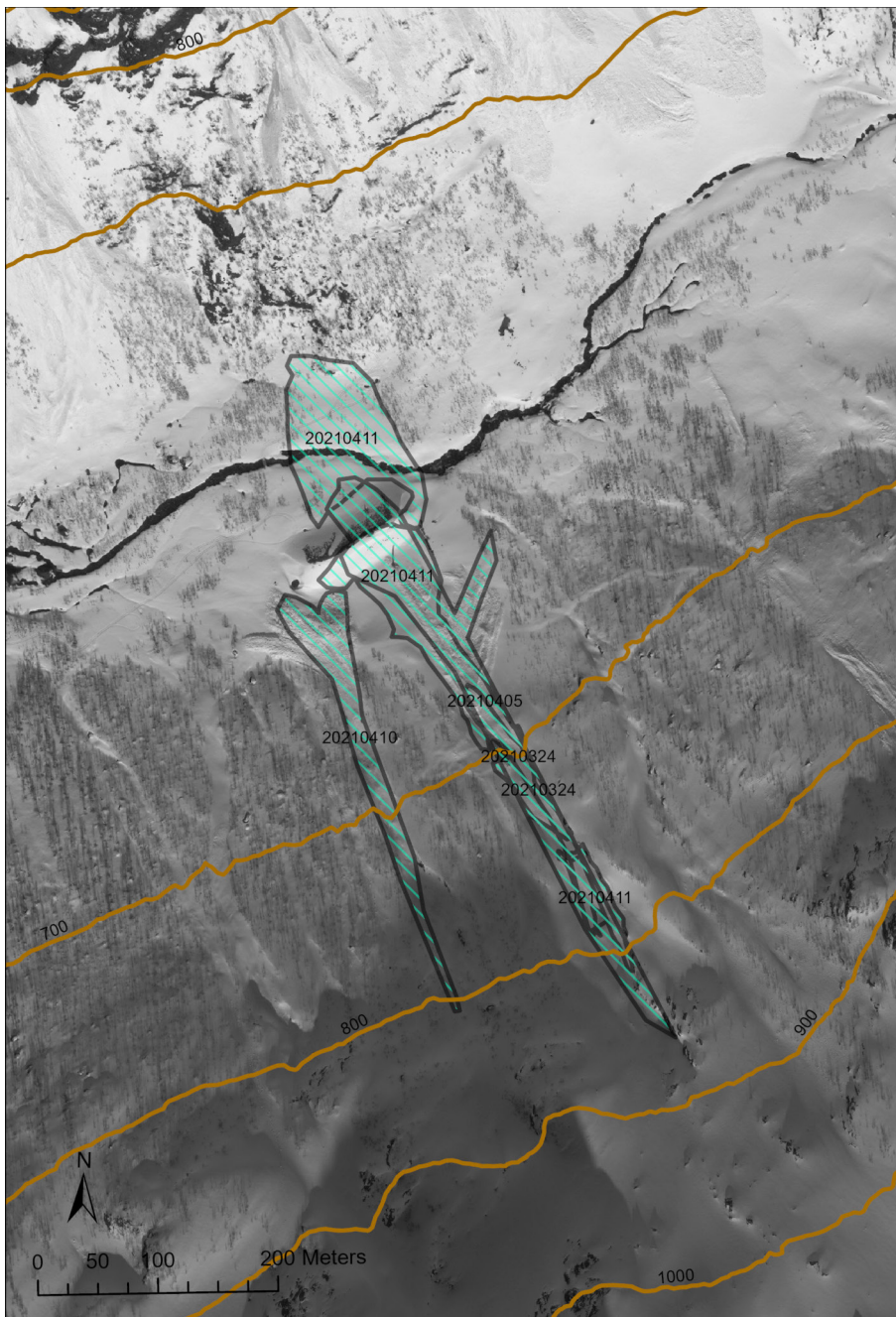


Figure 9 Timing of the avalanche radar distance versus frontal arriving time  $t_f$ .

## Deposition area



*Figure 10 Avalanche track with deposition area approximately five weeks after the avalanche event 2021-04-11 (photo Krister Kristensen 2021-05-21).*



*Figure 11 Deposition area of three natural avalanche events in 2021 based on brief field surveys; dates of the events are indicated.*

**2021-02-18T21:43 (CET)**

A moving target identification (MTI) plot is depicted in Figure 12.

20210218T214336\_651\_alarm\_0\_:

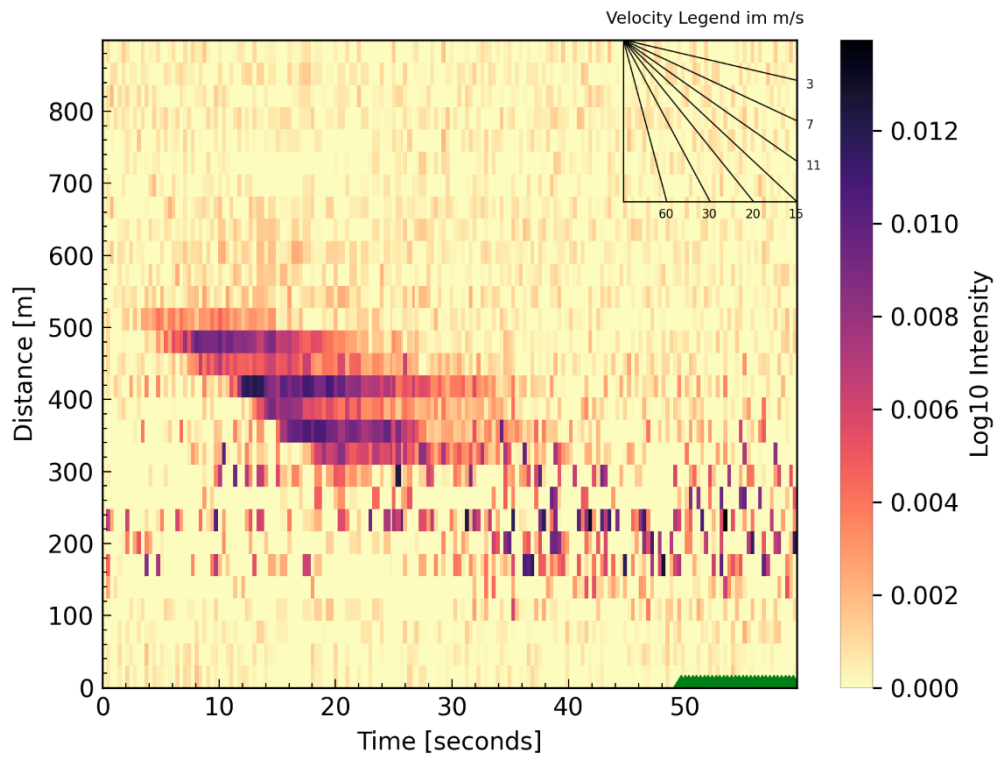


Figure 12 MTI data (Radar distance = Distance + 176.8 m).

No data available from the other systems.

**2021-03-20T16:35 (CET)**

A moving target identification (MTI) plot is presented in Figure 13.

20210320T153455\_4504\_alarm\_0\_:

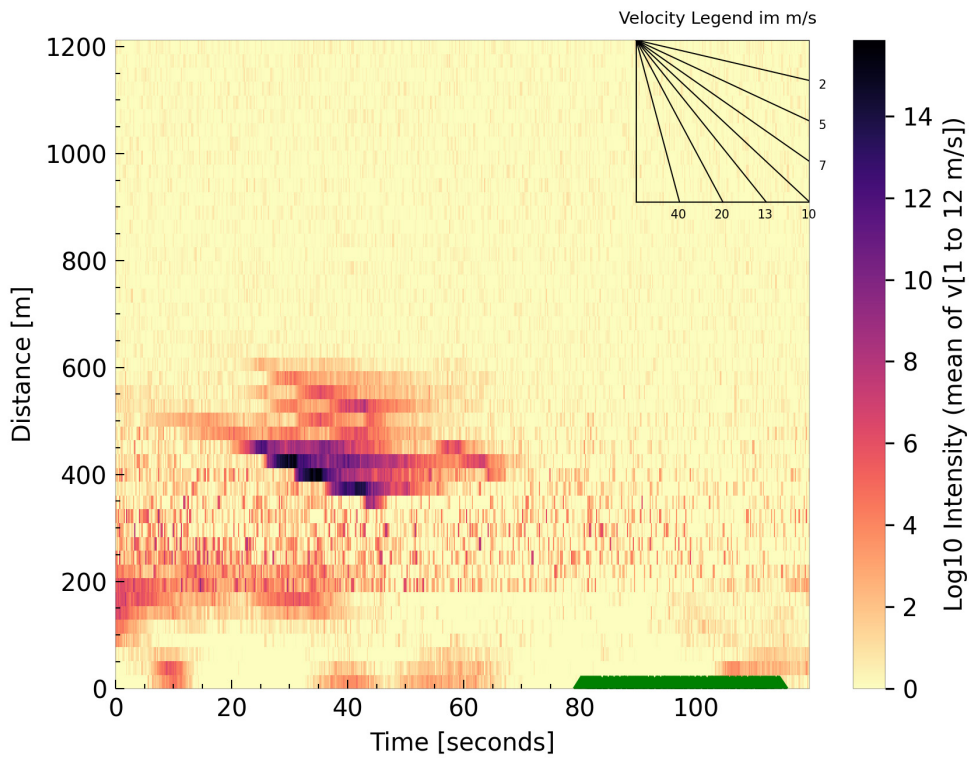


Figure 13 MTI data (Radar distance = Distance + 176.8 m).

No data available from the other systems.

**2021-03-24T22:11 (CET)**



Figure 14 Release area after natural release on 2021-03-24 around 22:09 (photo 2021-03-25 07:59)



Figure 15 Image of the runout area before (2021-03-24 22.00) and after the release (2021-03-24 22:30). Deposits are indicated by the red line in the right photo.

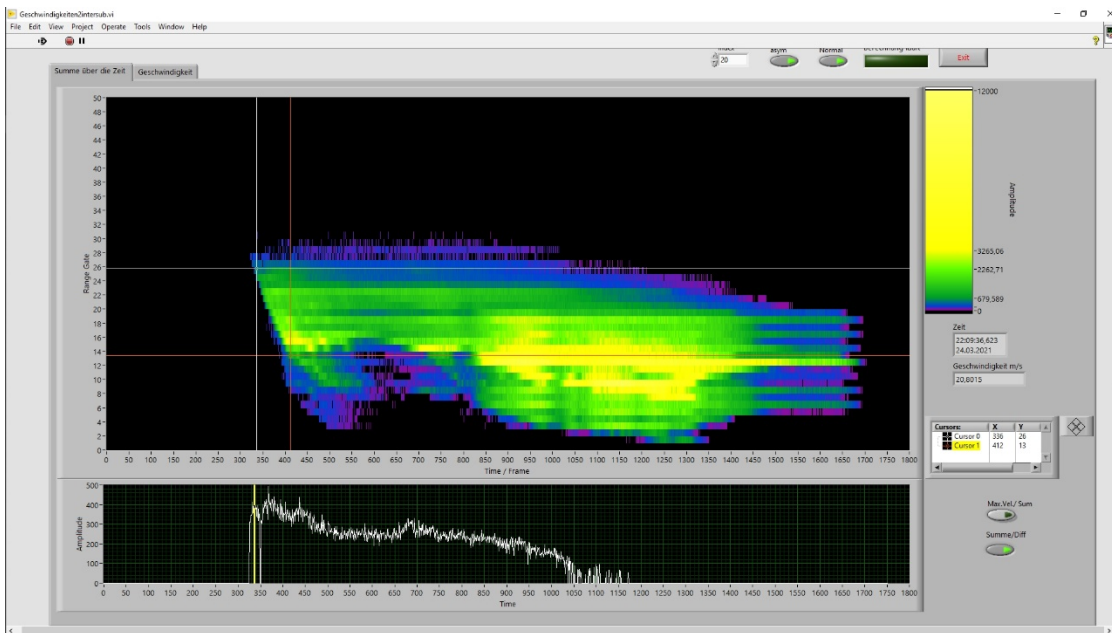


Figure 16 Radar data (Radar distance = Distance + 176.8 m).

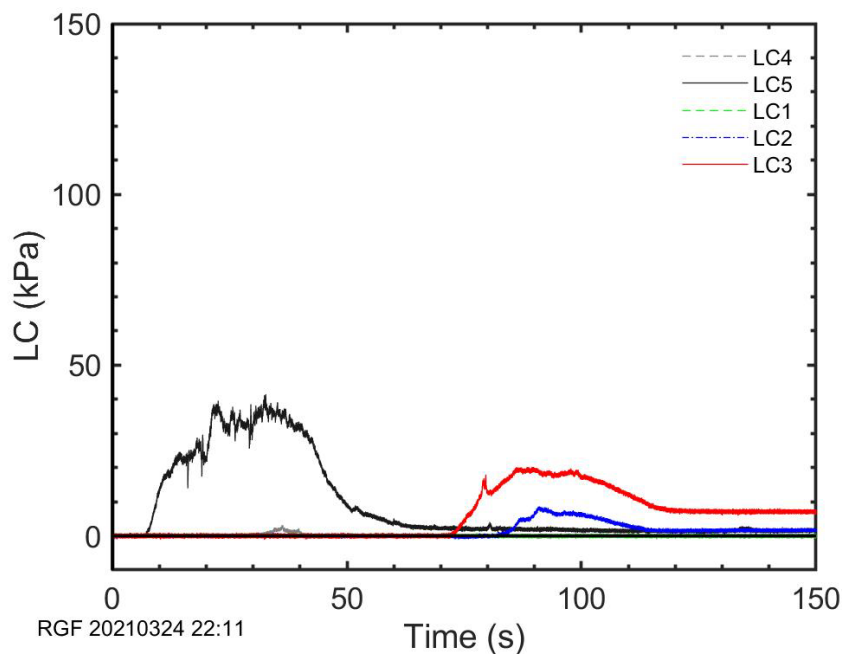


Figure 17 Load cell measurement: pressure vs. time at the position of the tower (LC45) and the concrete wedge (LC123).

2021-04-05T07:01 (CET)

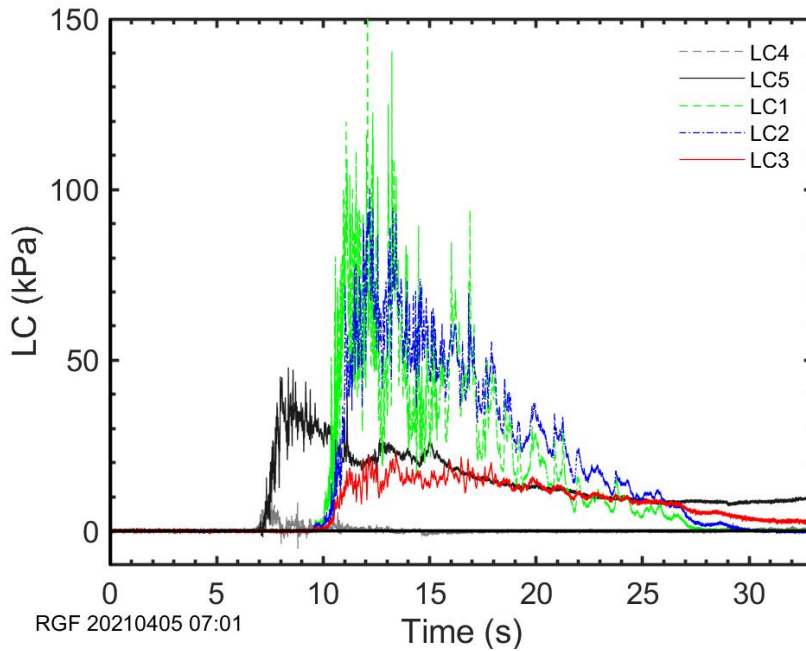


Figure 18 Load cell measurement: pressure vs. time at the position of the tower (LC45) and the concrete wedge (LC123).



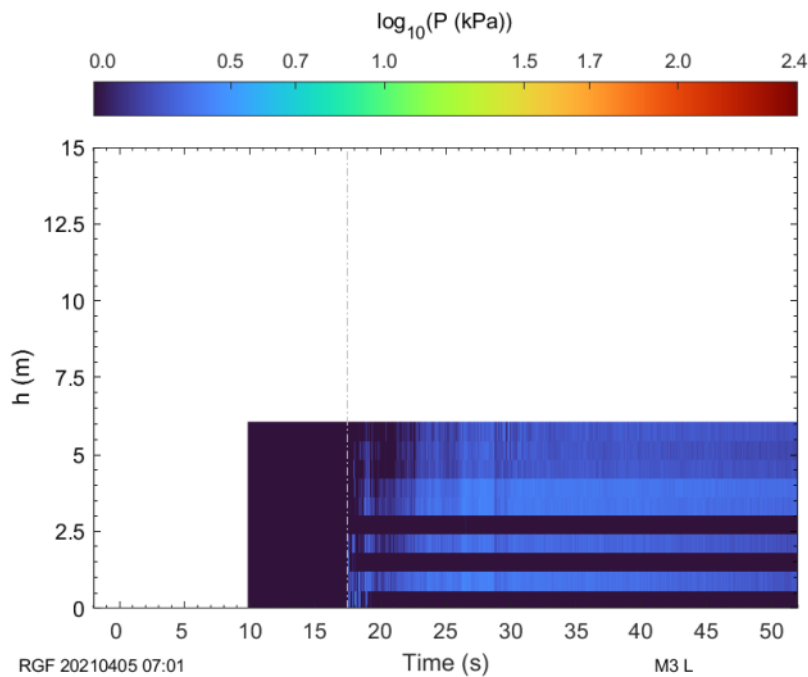
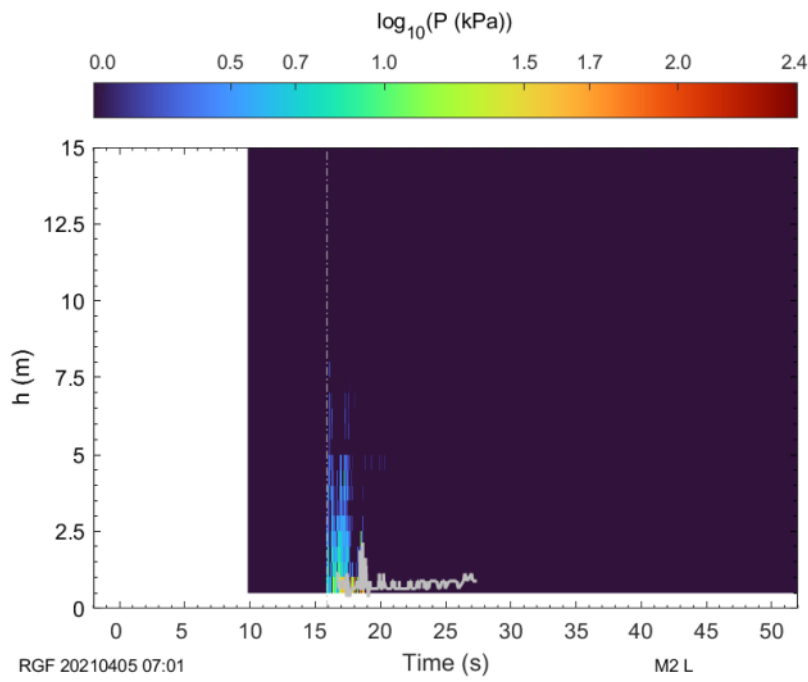


Figure 19 Load cell measurement: pressure ( $\log_{10}(P)$ ) vs. time at the position of mast M2 (top grey line indicates flow height derived from switches) and mast M3 (bottom).

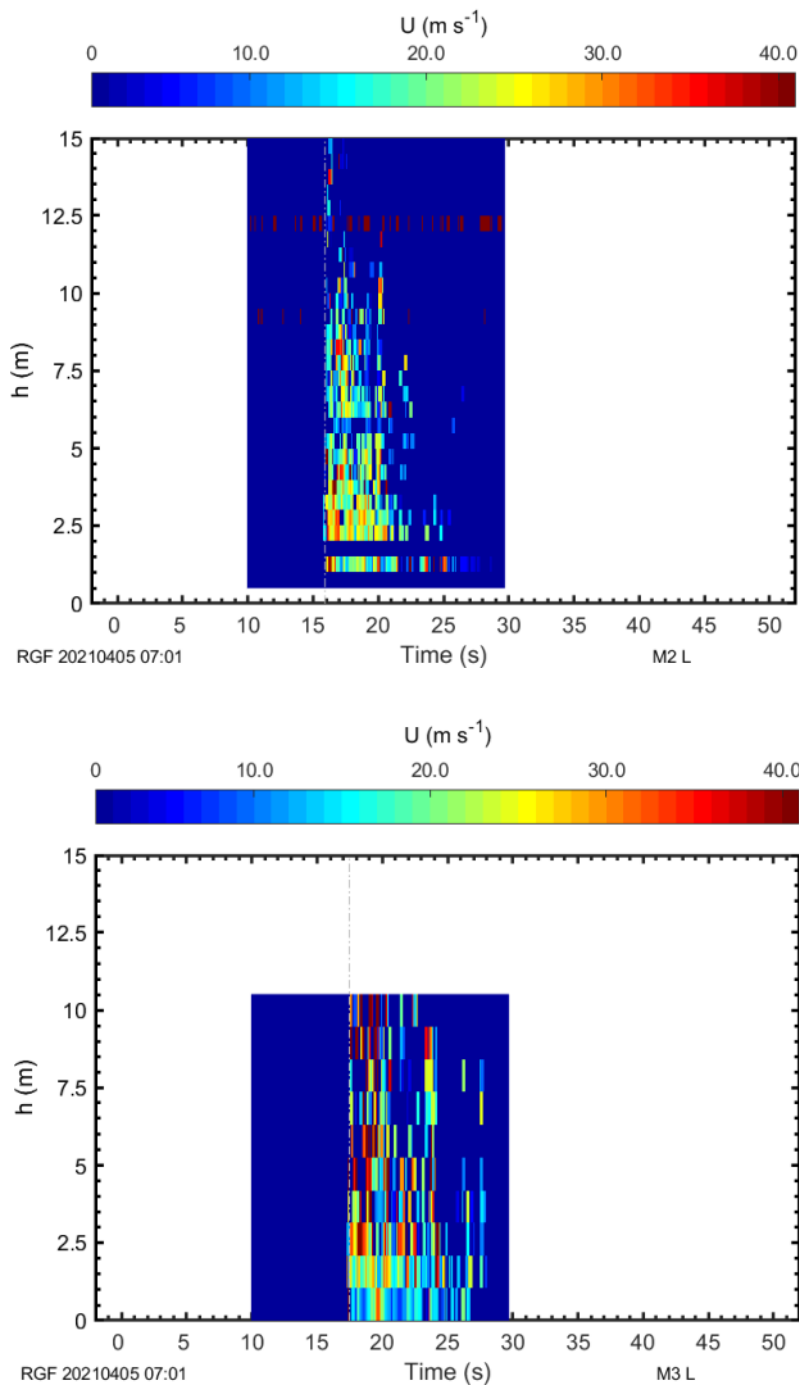


Figure 20 Velocity estimates derived from LED-sensors at mast M2 (top) and mast M3 (bottom).

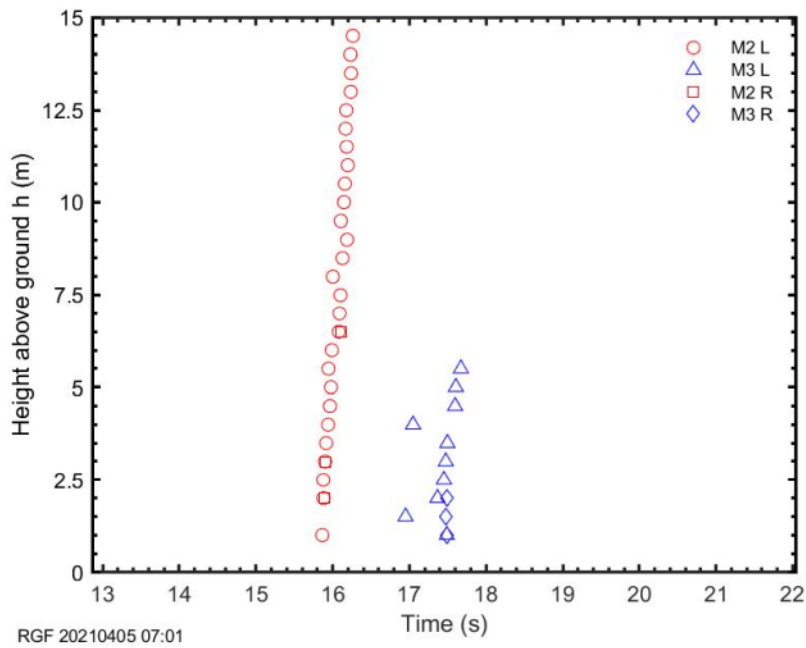


Figure 21 Frontal arriving time at mast M2 and mast M3.

2021-04-06T06:14 (CET)

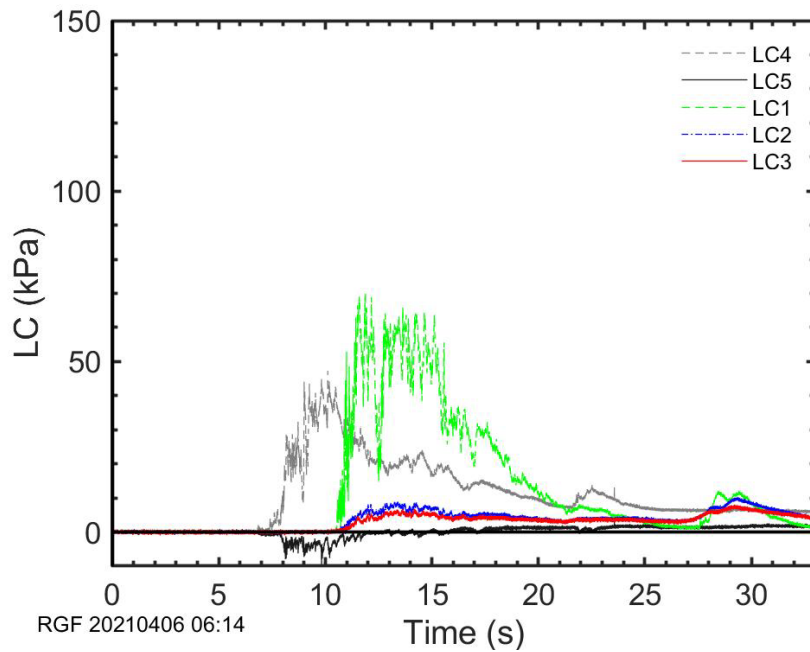


Figure 22 Load cell measurement: pressure vs. time at the position of the tower (LC45) and the concrete wedge (LC123).

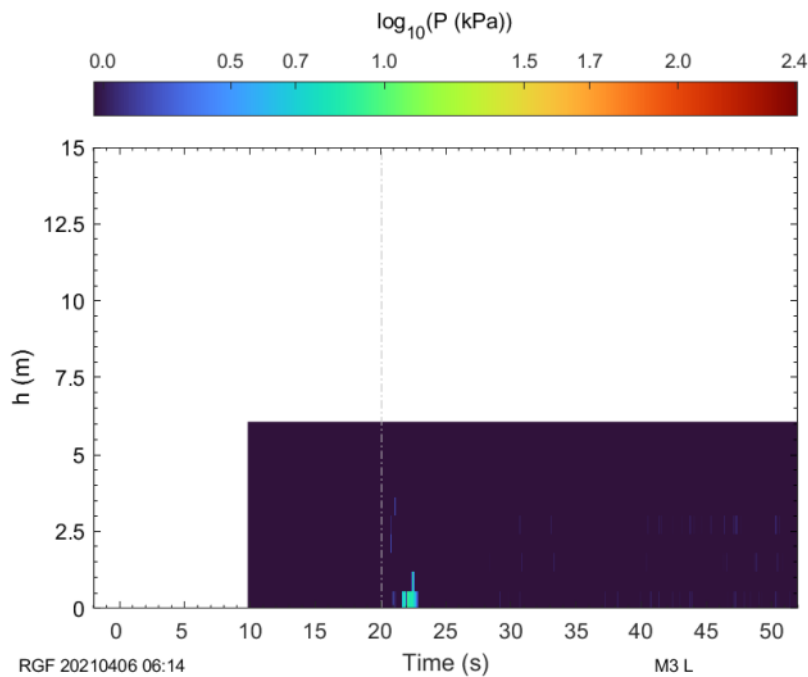
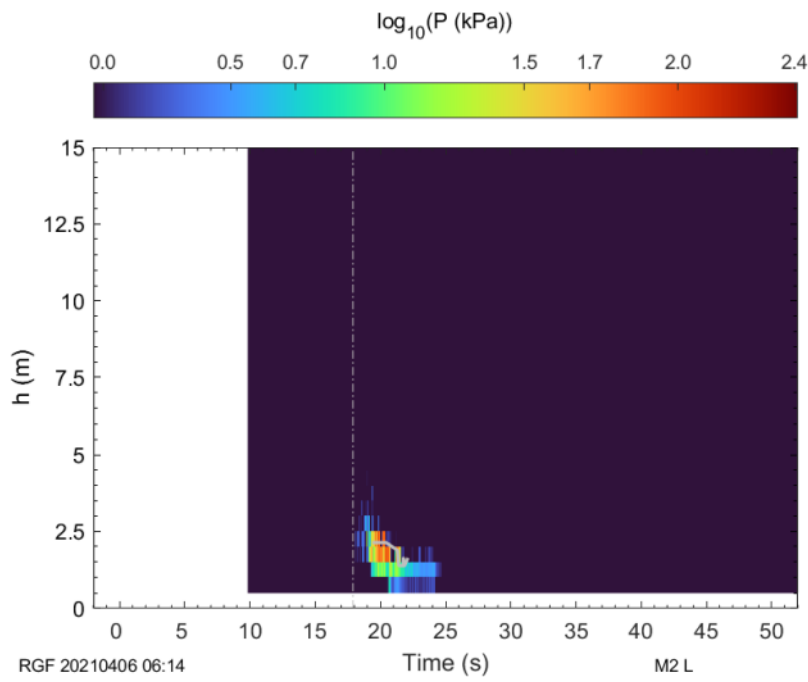


Figure 23 Load cell measurement: pressure ( $\log_{10}(P)$ ) vs. time at the position of mast M2 (top, grey line indicates flow height derived from switches) and mast M3 (bottom).

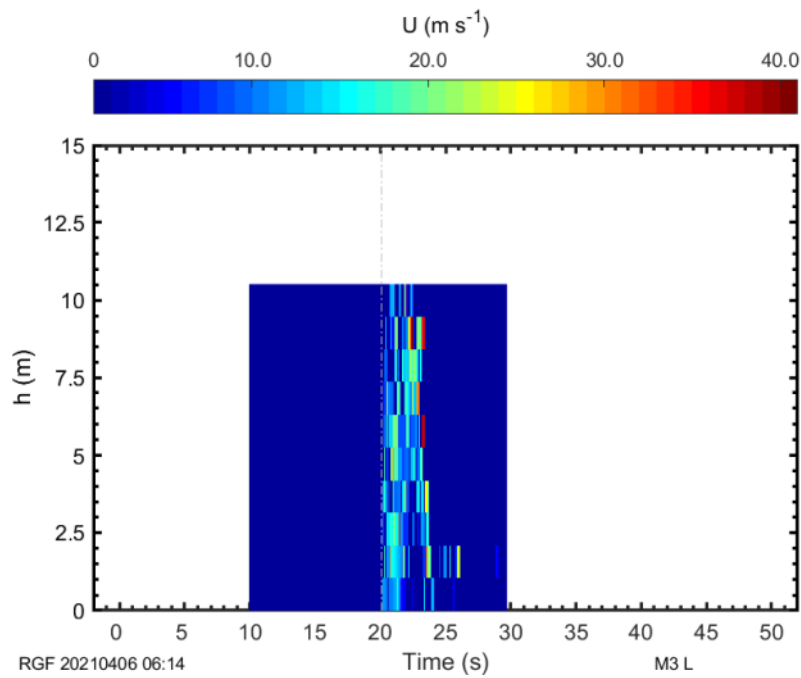
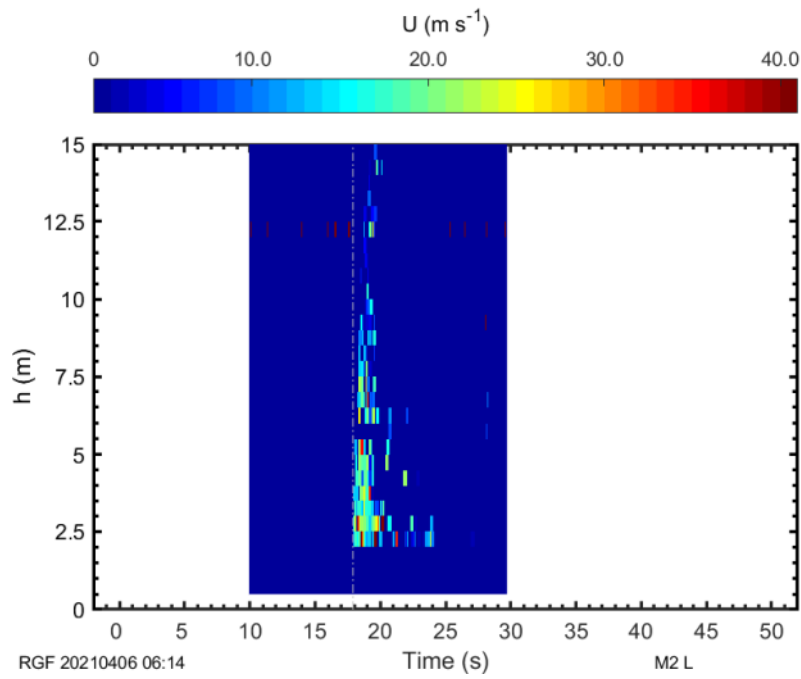


Figure 24 Velocity estimates derived from LED-sensors at mast M2 (top) and mast M3 (bottom).

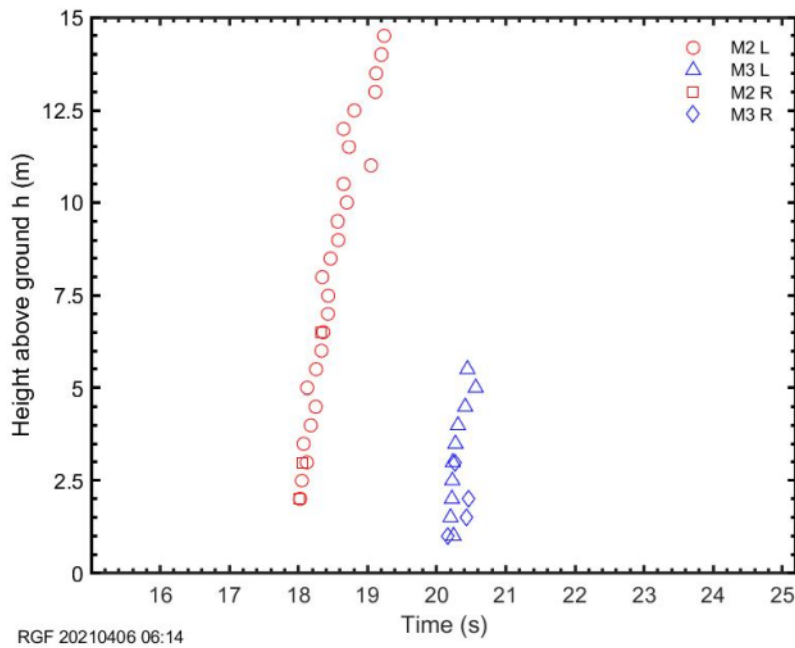


Figure 25 Frontal arriving time at mast M2 and mast M3.

2021-04-10T01:53 (CET)

20210409T235611\_all\_alarm\_35\_:

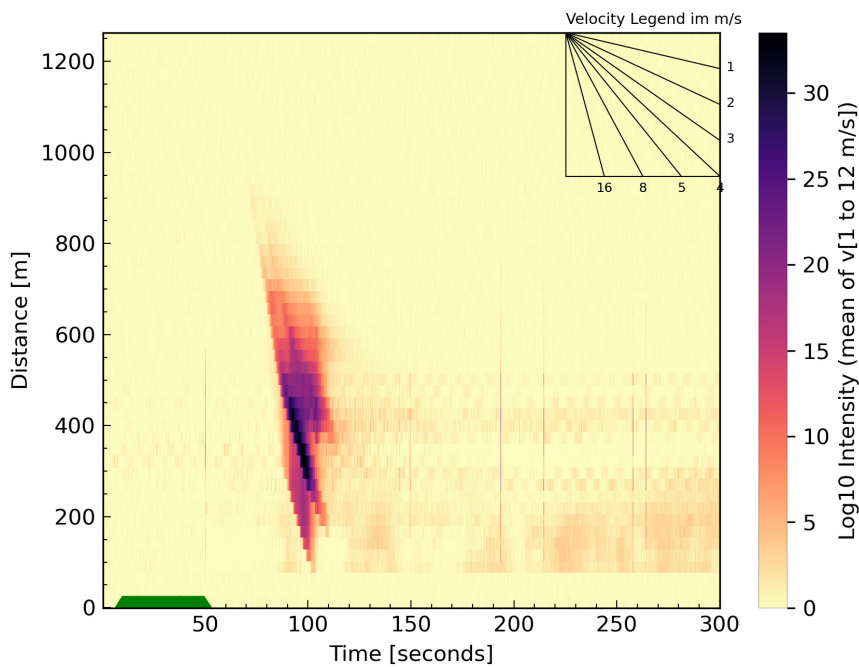


Figure 26 MTI data (Radar distance = Distance + 176.8 m).

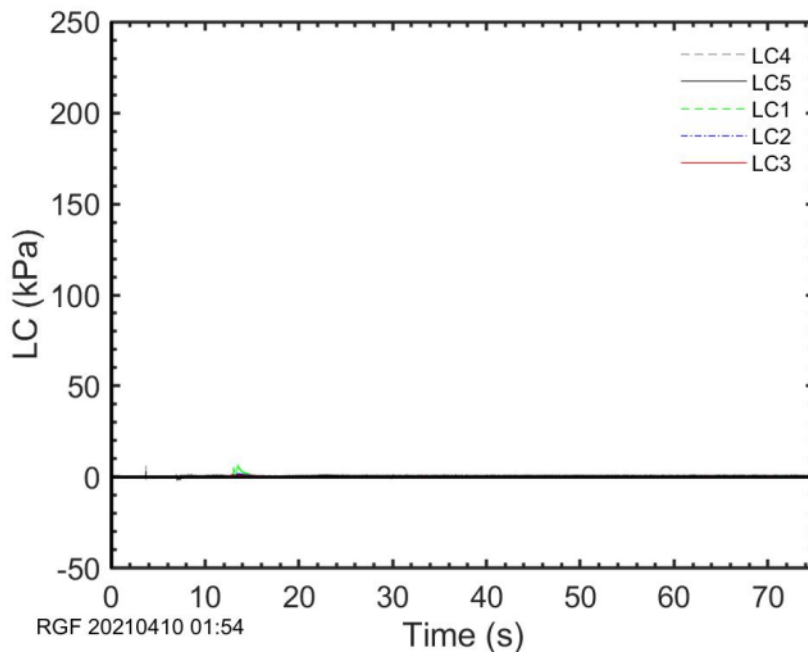


Figure 27 Load cell measurement: pressure vs. time at the position of the tower (LC45) and the concrete wedge (LC123).

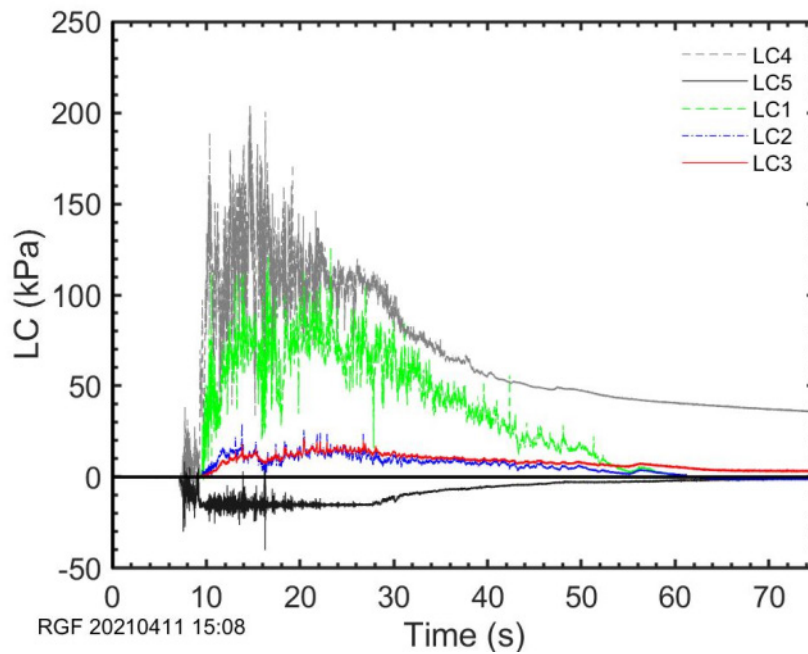


Figure 28 Load cell measurement: pressure vs. time at the position of the tower (LC45) and the concrete wedge (LC123).

2021-04-11T15:07 (CET)



*Figure 29 Release area after artificial release on 2021-04-11*



*Figure 30 Deposition area after artificial release on 2021-04-11*



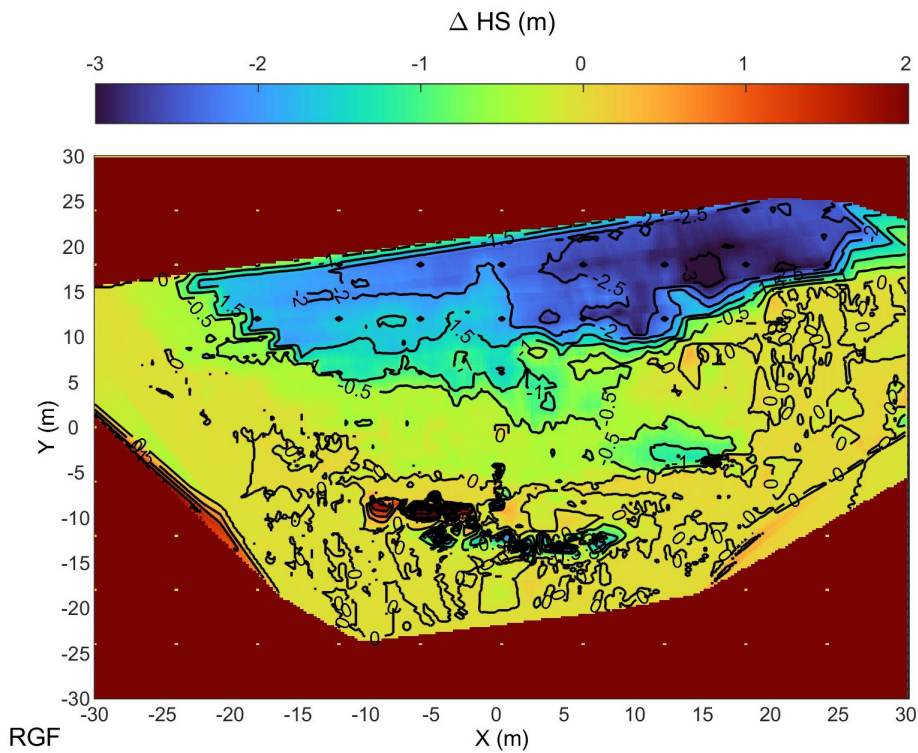


Figure 31 Vertical  $\Delta HS$  in parts of release area after artificial release on 2021-04-11. Location of the trigger point is at  $[X,Y]=[0,0]$ .

20210411T130625\_c2\_alarm\_107\_:

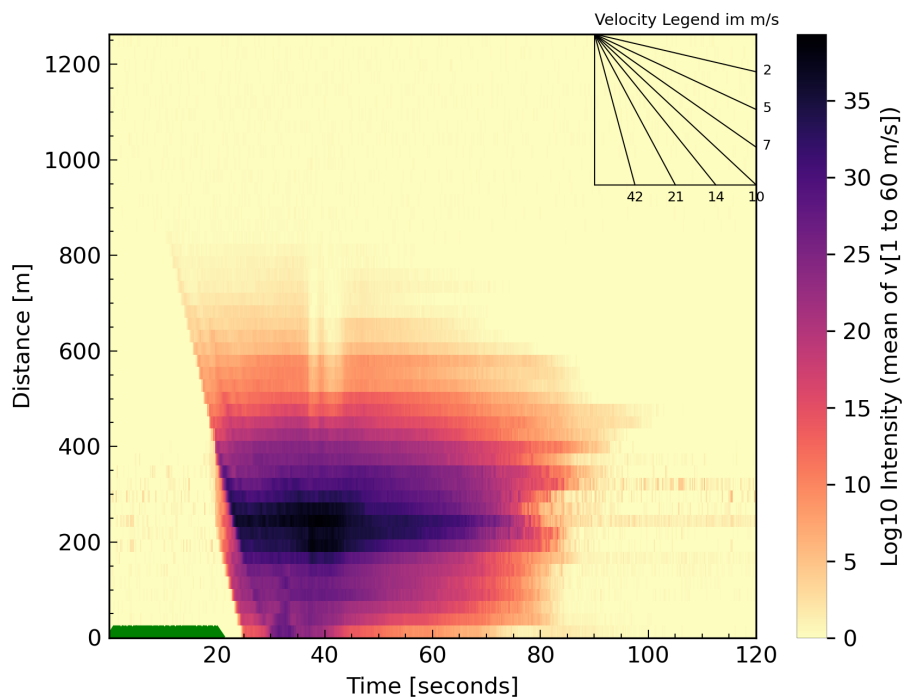


Figure 32 MTI data (Radar distance = Distance + 176.8 m).

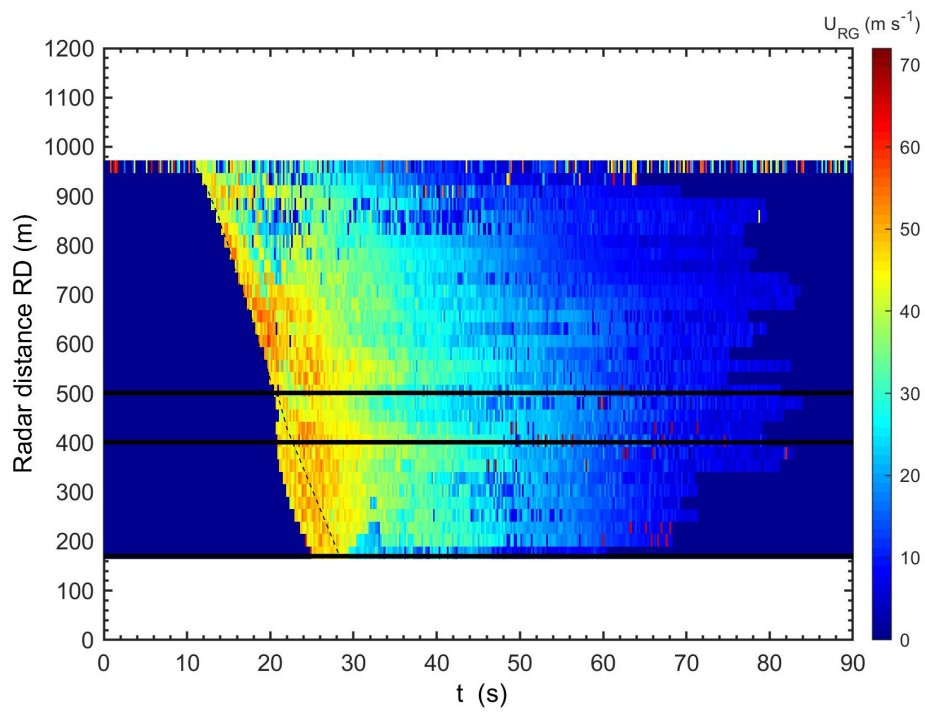


Figure 33 Maximum velocity measured at the range gates over time, t.

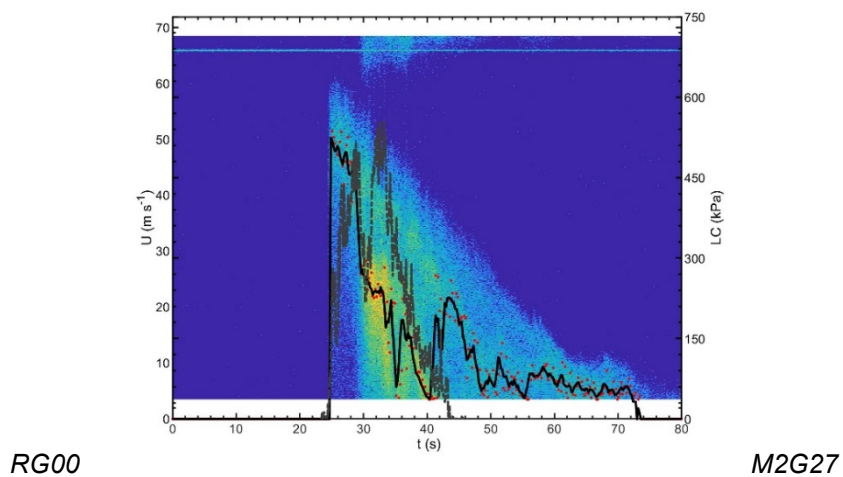
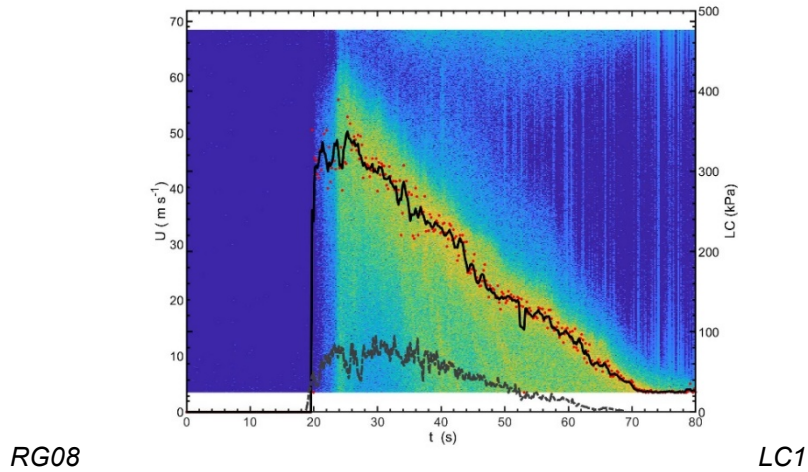
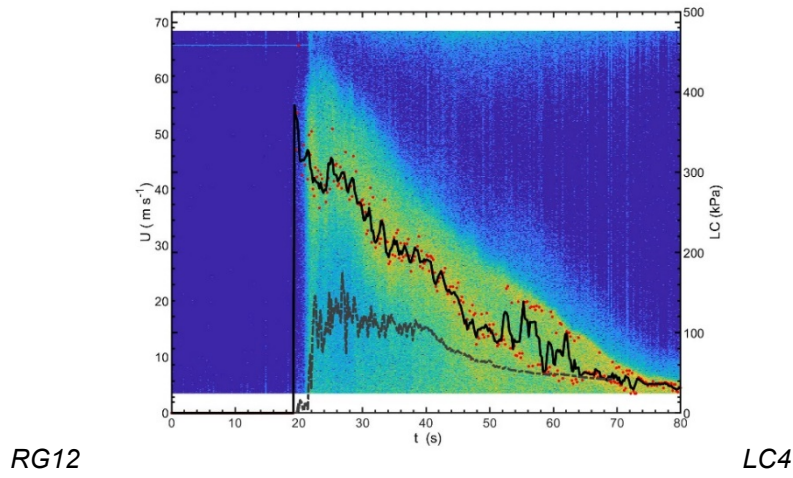


Figure 34 Echo intensity spectra from pulsed Doppler-radar measurements. The red-dots and the black line indicate the velocity at maximum echo intensity. The gray lines show the pressure measurements at load cell LC4, LC1 and M2G27. Data are smoothed.

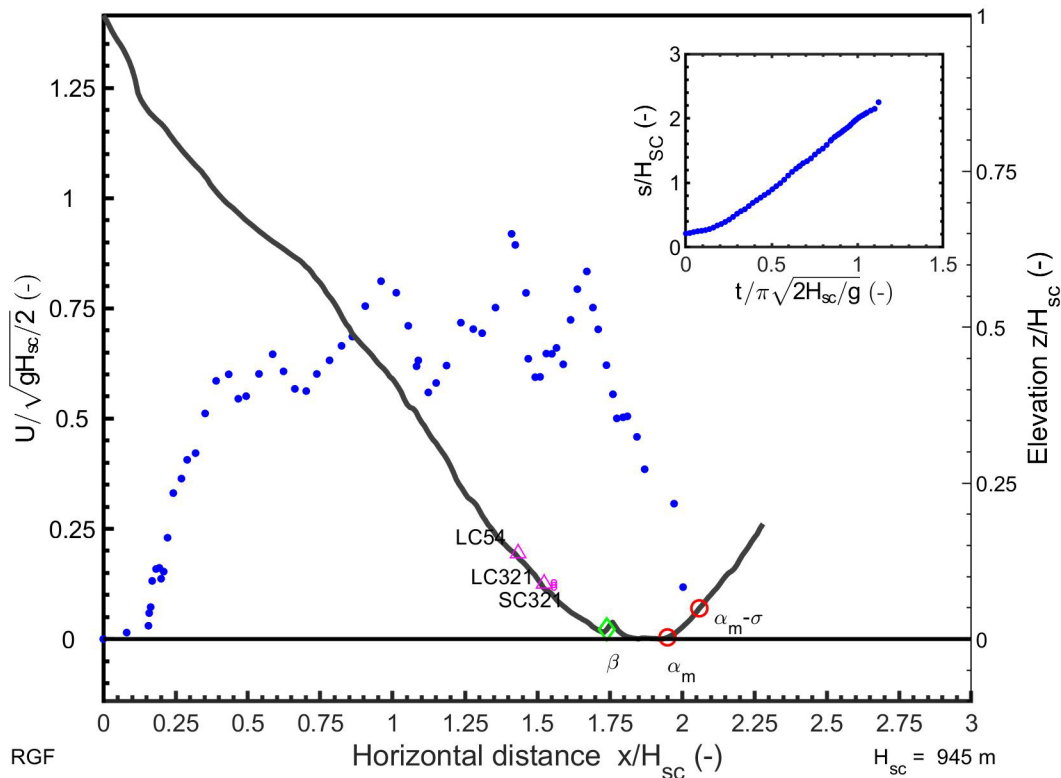


Figure 35 Velocity estimates along the track derived from video footage.

Table 2 Estimated mass balance

	Area (proj.) (m <sup>2</sup> )	HS (vert.) (m)	Volume (m <sup>3</sup> )	Density (kg m <sup>-3</sup> )	Mass (10 <sup>6</sup> kg)
Release	11200	1.5		200	2.9
	2200	1		200	0.4
Track	60000	<b>0.3</b>		150	
Deposition			16448	450	7.4

### Drone-based digital mapping

The 11.04.2021 avalanche experiment was also monitored by drone to support mapping of snow erosion, deposit and calculation of mass balance. An automated drone survey methodology was successfully deployed to map the lower portion of the avalanche path, both before and after the experiment, as well as in a snow-free condition (in summer). Furthermore, a pre-avalanche snow height map was produced based on a comparison with the snow-free terrain model. Additionally, a drone was used as a hovering camera in the valley to record video of the avalanche.

Digital snow surface models were constructed for geospatial analysis using a directly georeferenced Structure-from-Motion photogrammetry workflow to the combined total of 800 individual drone images. As listed in Table 2, a total mobilized snow volume of

approximately 16,500 m<sup>3</sup> was estimated from the difference between the pair of independently georeferenced snow surface models (before, after the event, as depicted in Figure 36, Figure 37, Figure 38) while orthomosaics provided high-resolution overviews of the avalanche path (Figure 39, Figure 40).

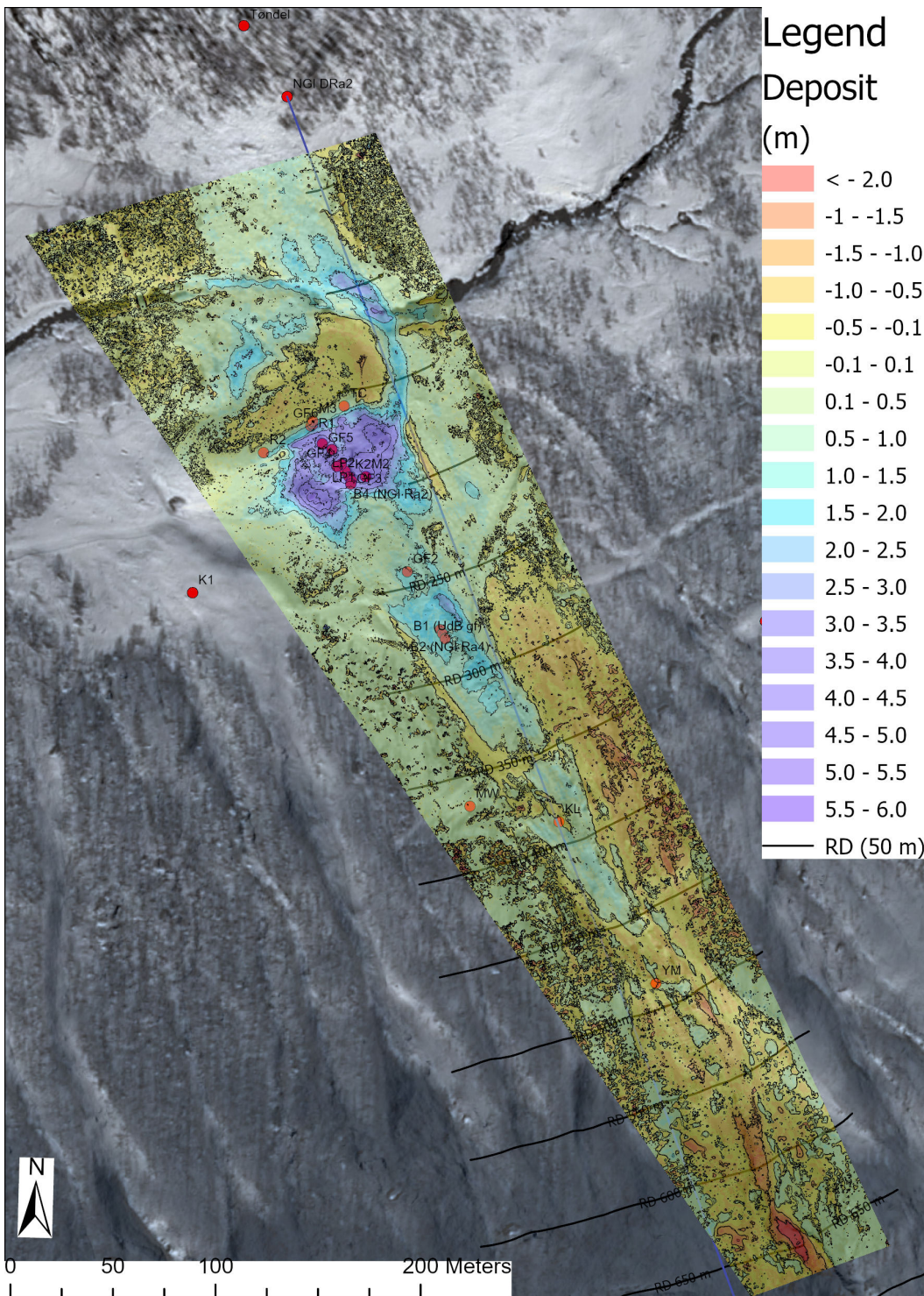


Figure 36 Estimated deposition pattern derived from drone survey.

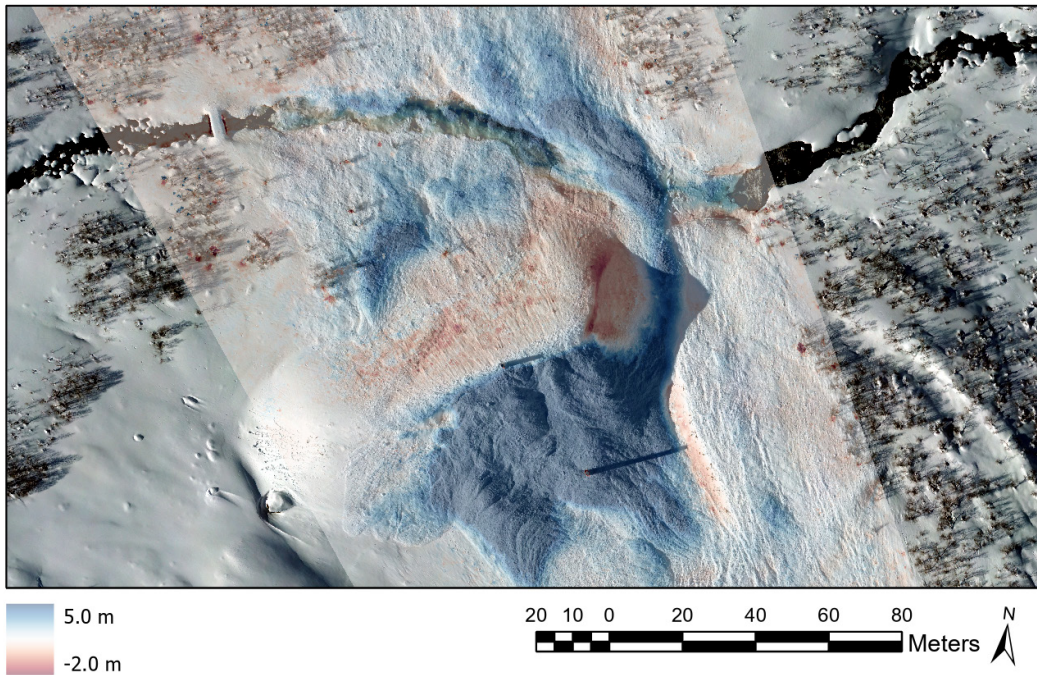


Figure 37 Comparison of drone image-derived elevation models generated from pre- and post-avalanche images; deposition around the retaining dam. Scale in vertical meters.

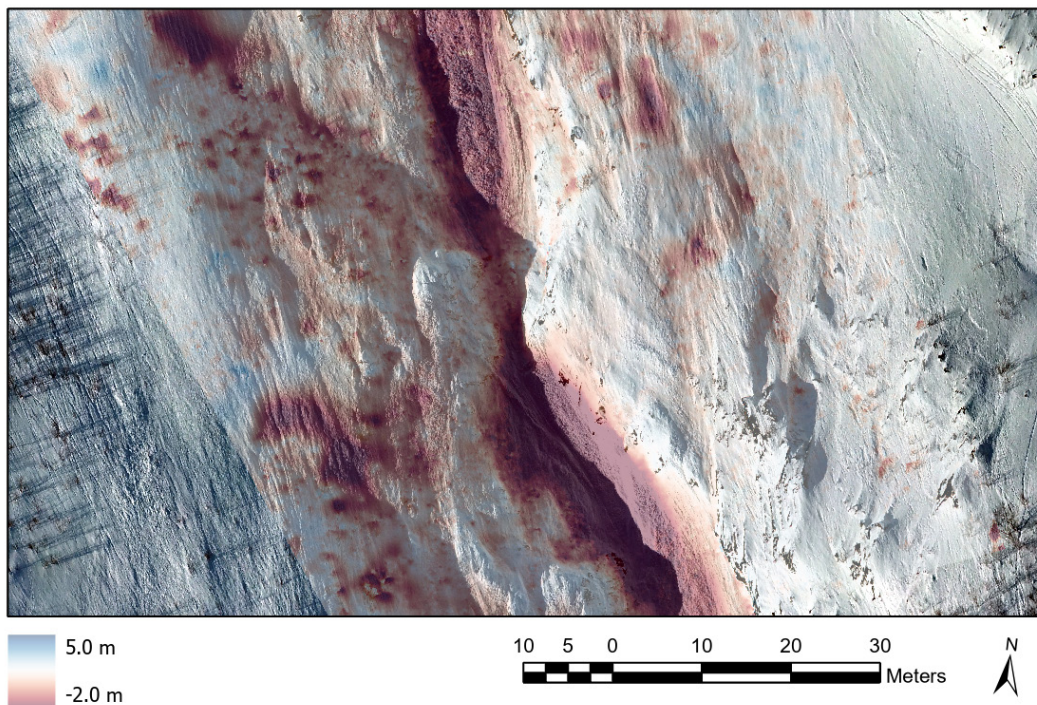


Figure 38 Comparison of drone image-derived elevation models generated from pre- and post-avalanche images; erosion areas along the avalanche path. Scale in vertical meters.

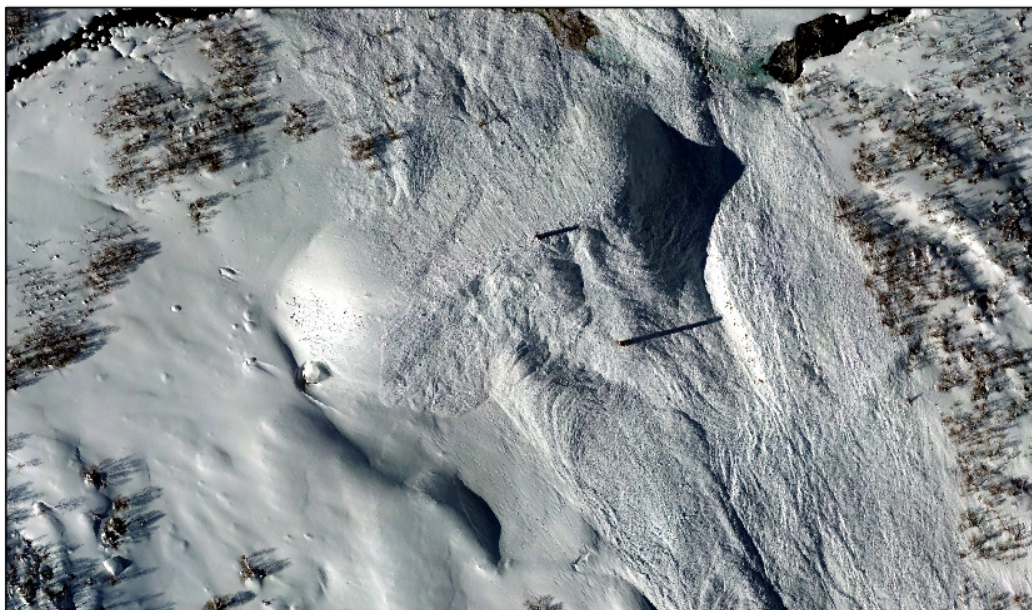


Figure 39 Drone image-derived orthomosaic of the retaining dam before (top) and after (bottom) the avalanche experiment on 11.04.2021.



Figure 40 Drone image-derived orthomosaic of the retaining dam in summer on 08.07.2021.

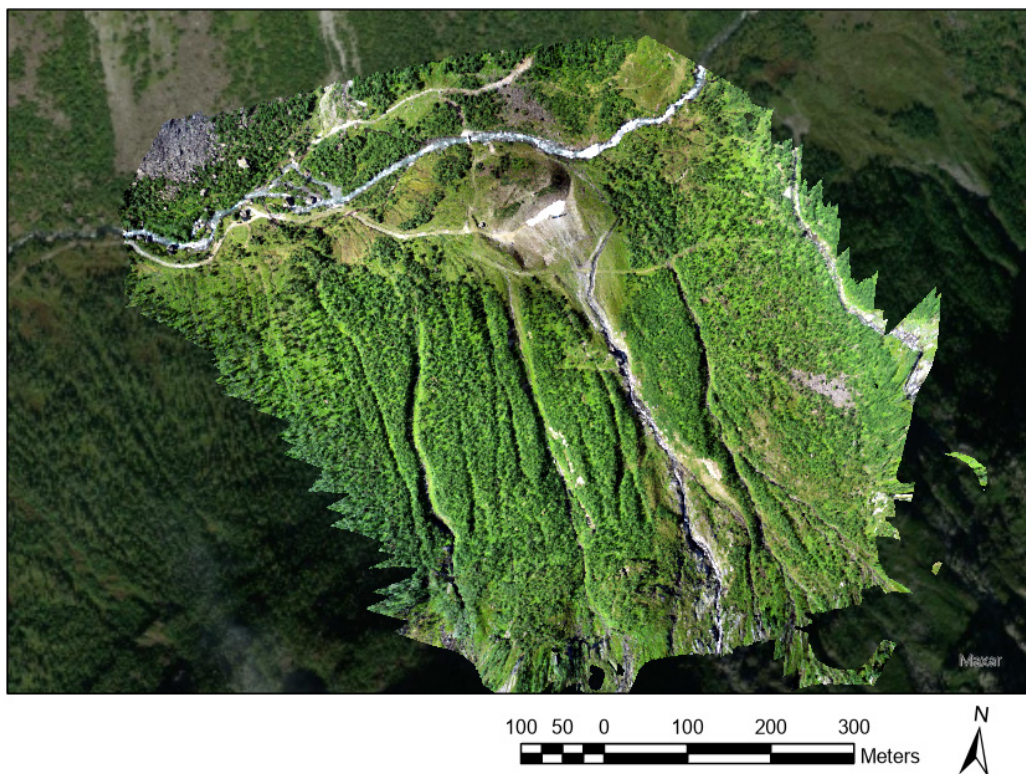


Figure 41 Drone image-derived orthomosaic raster product with a spatial resolution of 7-cm per pixel for summer survey on 08.07.2021.





Figure 42 Drone image-derived orthomosaic close-up of the instrumented mast (M3) on the retaining after the avalanche experiment on 11.04.2021 (top) and in summer on 08.07.2021 (bottom).

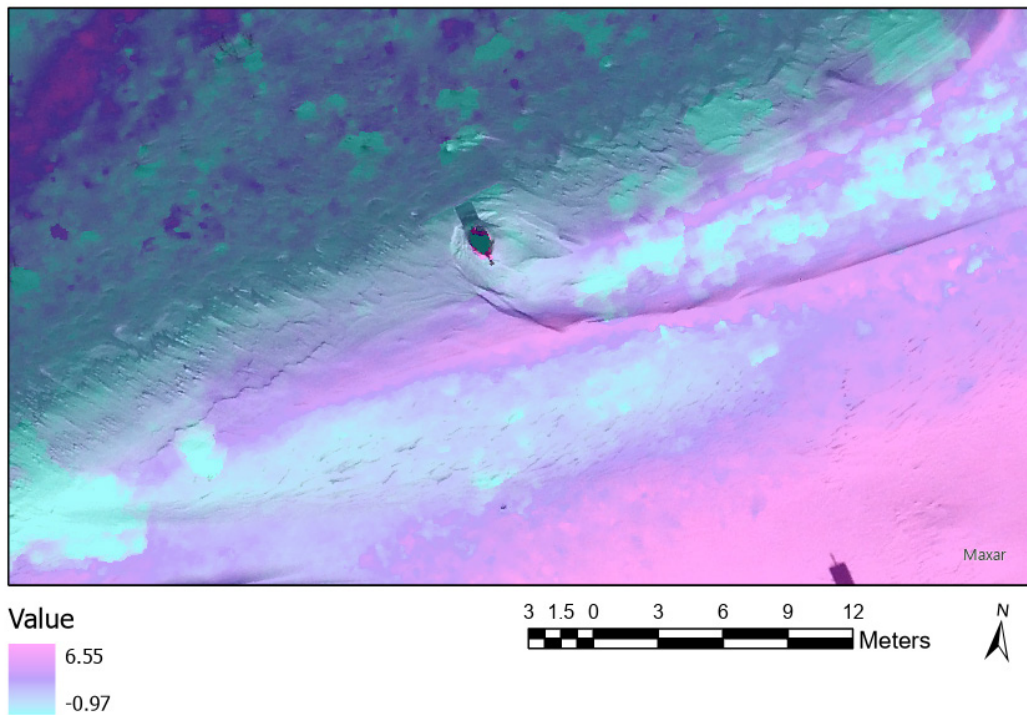


Figure 43 Comparison of drone image-derived elevation models generated from pre-avalanche images and summer (bare ground) images. Scale in vertical meters.

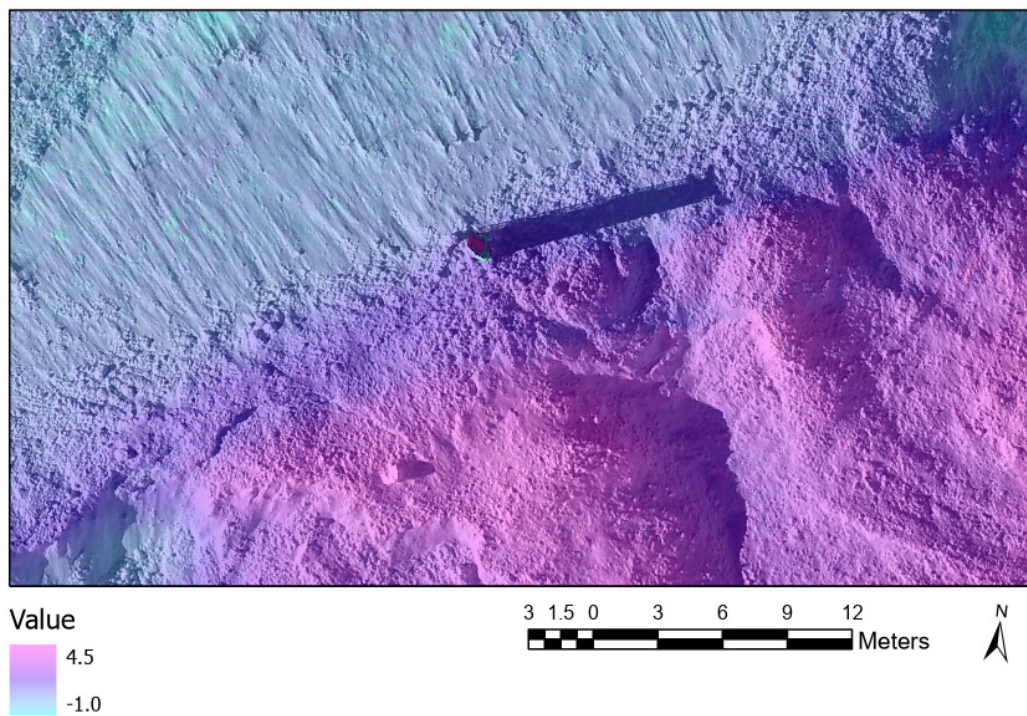


Figure 44 Comparison of drone image-derived elevation models generated from pre-avalanche images and post-avalanche images. Scale in vertical meters.

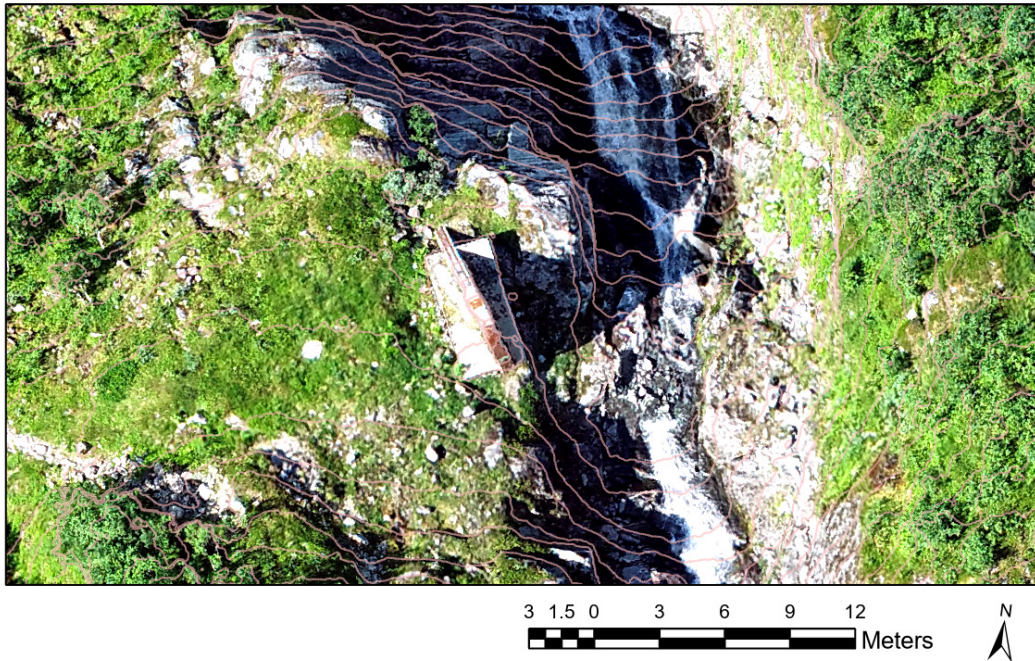


Figure 45 Drone image-derived orthomosaic around the concrete wedge; snow-free imagery from 08.07.2021. Contour lines at 1 meter intervals.

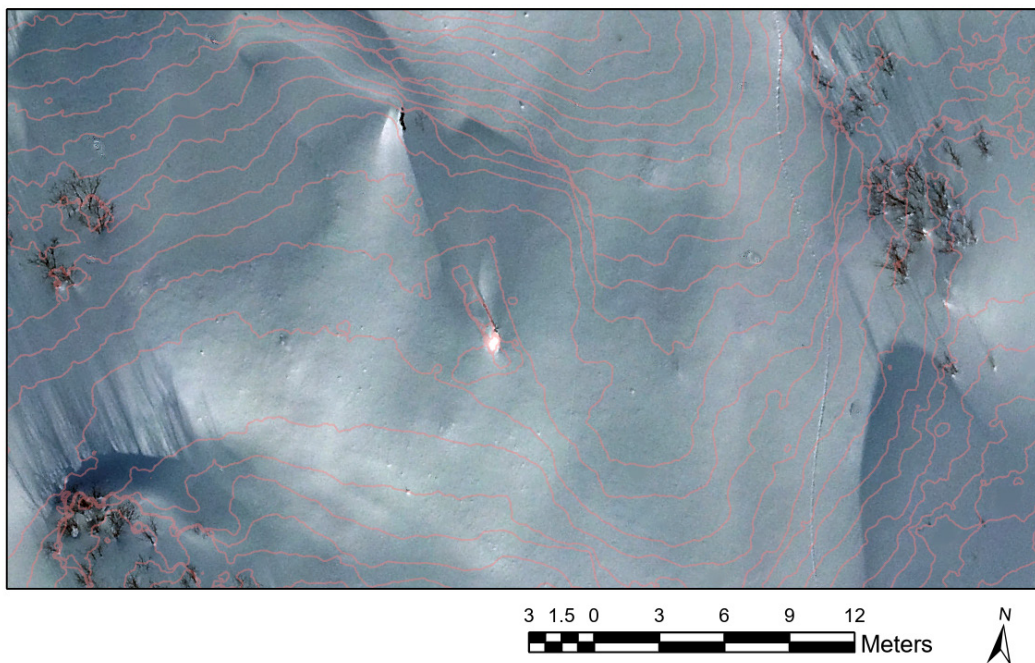


Figure 46 Drone image-derived orthomosaic around the concrete wedge prior to avalanche experiment on 11.04.2021 with contour lines from snow-free survey. Contour lines at 1 meter intervals.

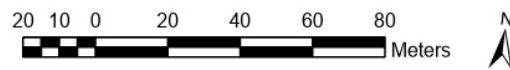
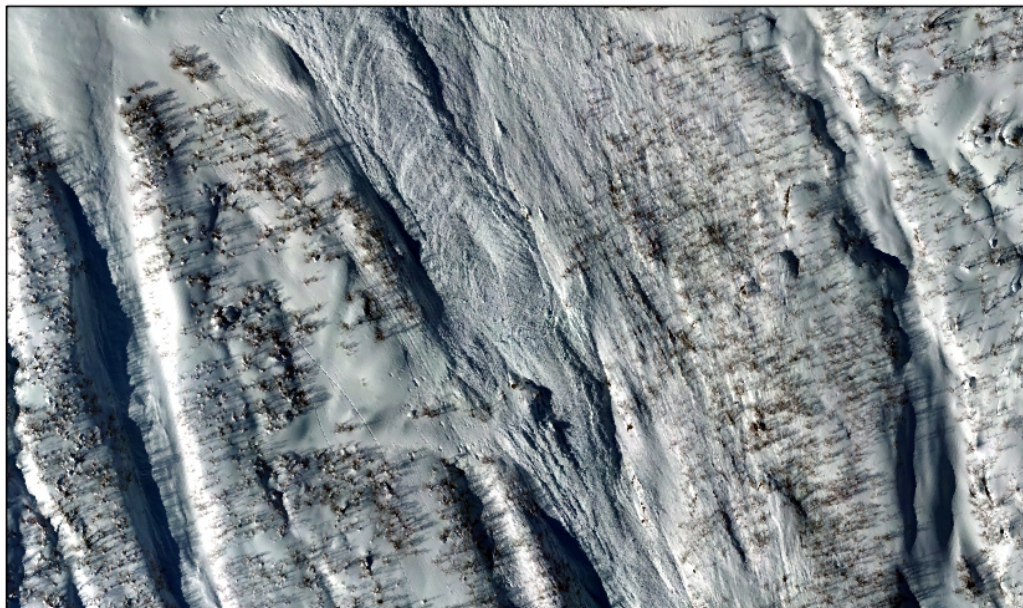
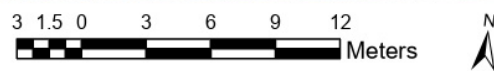
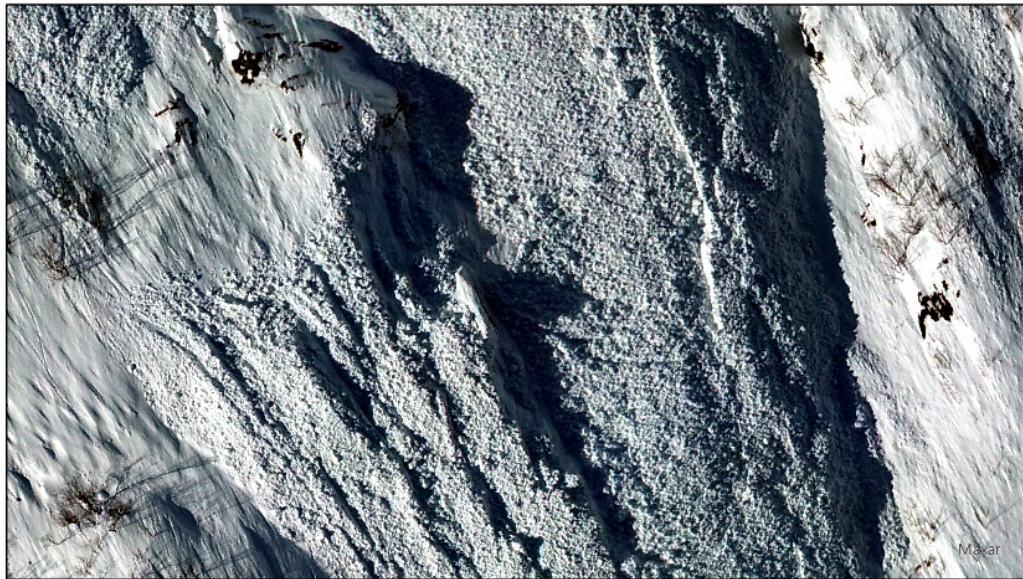


Figure 47 Drone image-derived orthomosaic close-up (top) and overview (bottom) of the concrete wedge after the avalanche experiment.

### Forest damage observations

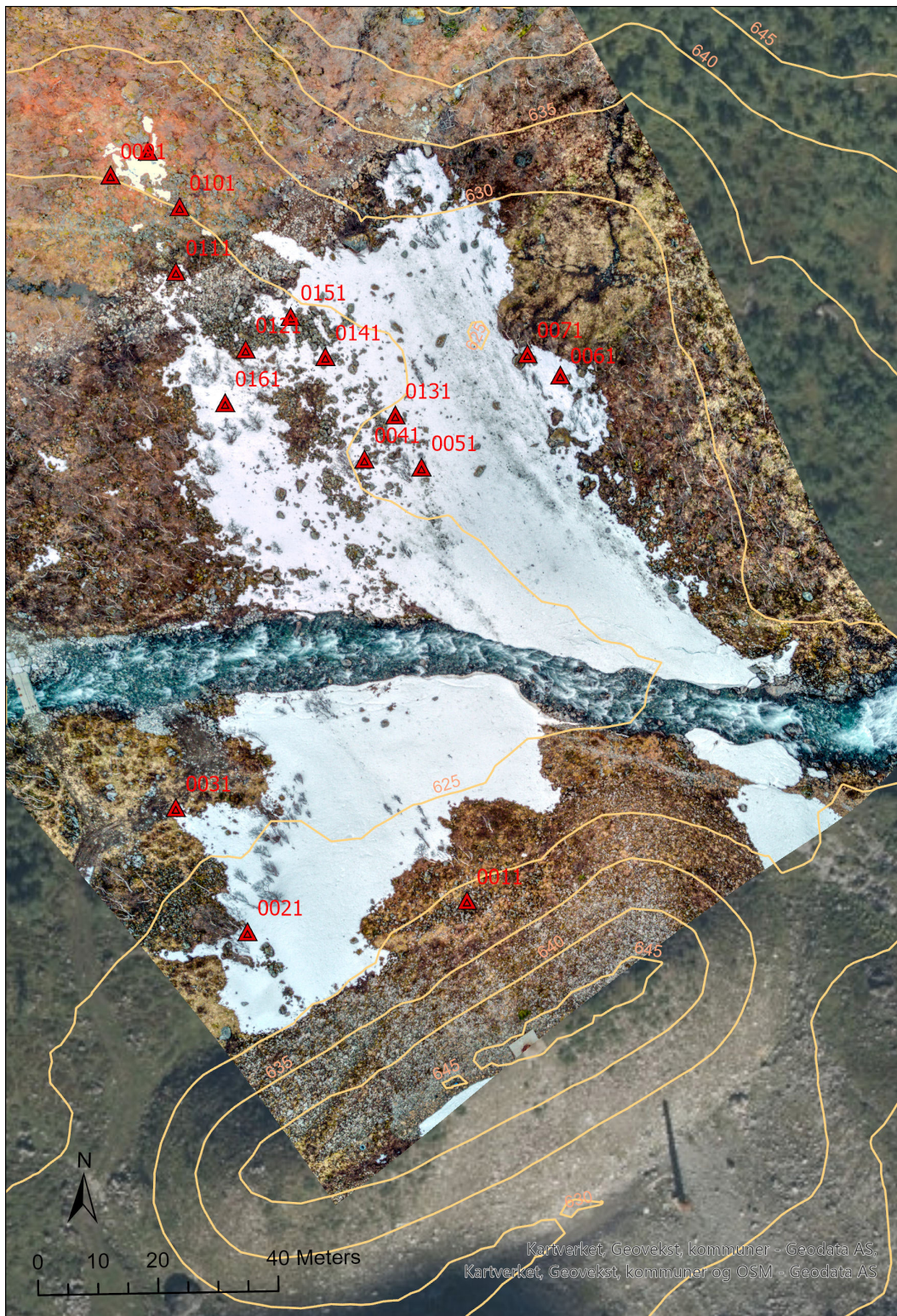


Figure 48 Deposition and forest damage locations (Photo Krister Kristensen 2021-05-21)



Figure 49 Point 11



Figure 50 Point 21



Figure 51 Point 31



Figure 52 Point 41



Figure 53 Point 51



Figure 54 Point 61



Figure 55 Point 71





Figure 56 Point 81



Figure 57 Point 91



*Figure 58 Point 101*



*Figure 59 Point 111*



*Figure 60 Point 121*



*Figure 61 Point 131*



*Figure 62 Point 141*

2021-05-02T12:54 (CET)

20210502T105443\_all\_alarm\_0\_:

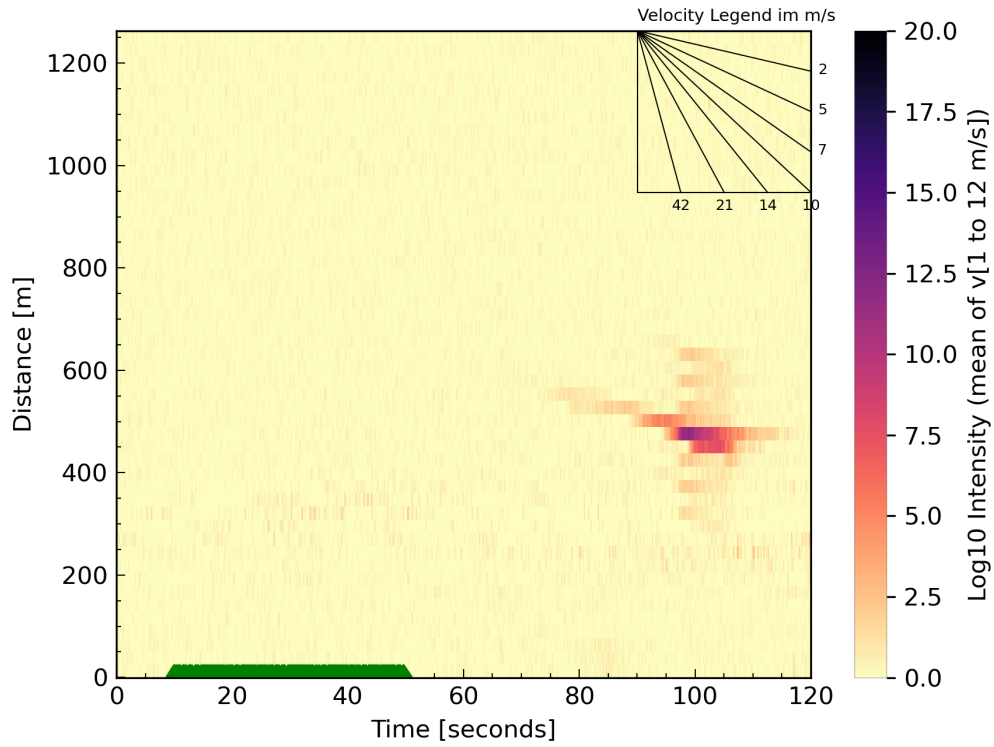


Figure 63 MTI data (Radar distance = Distance + 176.8 m).

2021-05-06T16:51 (CET)

20210506T145132\_all\_alarm\_0\_:

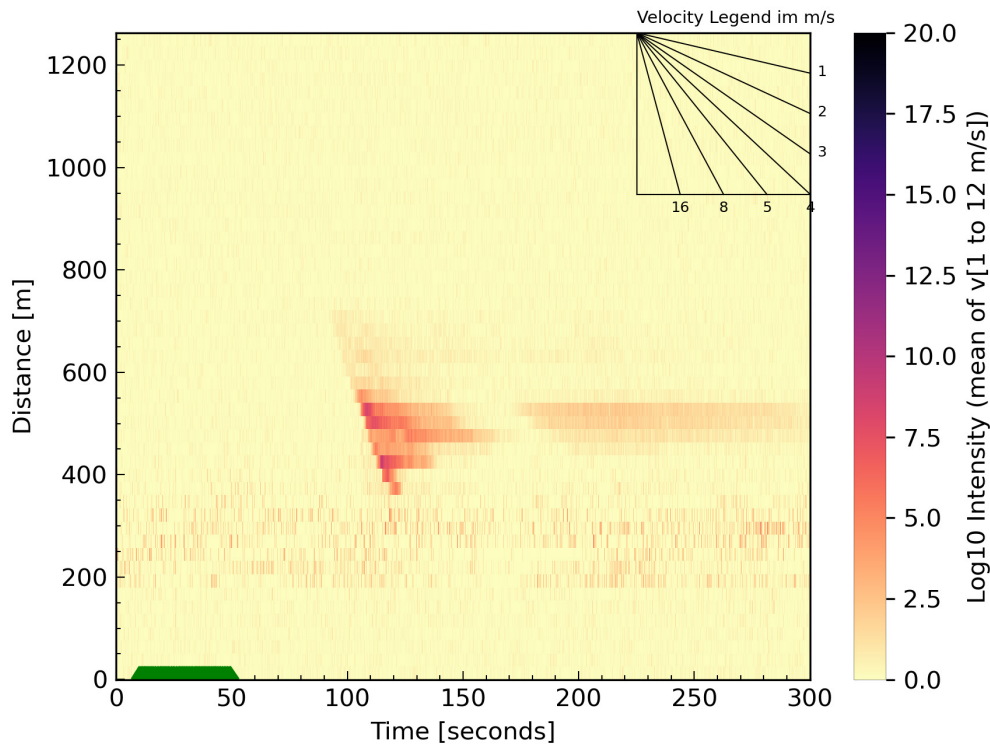


Figure 64 MTI data (Radar distance = Distance + 176.8 m).

## 5 Concluding remarks

With additional financial means through basic research funding (basisbevilgning), several instrument upgrades were established or prepared at the Ryggfonn test site in time for the 2020/2021 winter season. Two small weather stations were installed at the top and at the valley bottom to provide better information on the environmental conditions prior to and during avalanche releases. The upgrades also included a laser scanner for the release area and supporting infrastructure for an autonomous pulsed Doppler radar. The radar system was installed in early 2021 in cooperation with BFW (Innsbruck, Austria). Instrument data collected for natural releases and the 11.04.2021 experiment were presented along with preliminary analyses.

## 6 References

- Gauer, P.; Breien, H.; Issler, D.; Kristensen, K.; Kronholm, K.; Lied, E. & Lied, K. (2010) The upgraded full-scale avalanche test-site Ryggfonn, Norway, Proceedings of the International Snow Science Workshop, Lake Tahoe, CA, October 17-22, 2010, 2010, 747-752
- Gauer, P. & Kristensen, K. (2016) Four decades of observations from NGI's full-scale avalanche test site Ryggfonn---Summary of experimental results, Cold Regions Science and Technology, 2016 , 125 , 162-176
- Norem, H.; Kvisterøy, T. K. & Evensen, B. D. (1985), Measurements of avalanche speeds and forces: Instrumentation and preliminary results of the Ryggfonn project Annals of Glaciology, 1985, 6, 19-22

<b>Dokumentinformasjon/Document information</b>		
<b>Dokumenttittel/Document title</b> WP 2 – Full-scale experiments at Ryggfonn. Ryggfonn avalanche observations 2020/2021		<b>Dokumentnr./Document no.</b> 20200017-06-TN
<b>Dokumenttype/Type of document</b> Teknisk notat / Technical note	<b>Oppdragsgiver/Client</b> NVE	<b>Dato/Date</b> 2022-04-07
<b>Rettigheter til dokumentet iht kontrakt/ Proprietary rights to the document according to contract</b> Oppdragsgiver / Client		<b>Rev.nr.&amp;dato/Rev.no.&amp;date</b> 0 /
<b>Distribusjon/Distribution</b> ÅPEN: Skal tilgjengeligjøres i åpent arkiv (BRAGE) / OPEN: To be published in open archives (BRAGE)		
<b>Emneord/Keywords</b> Norwegian_avalanche_grant		

<b>Stedfesting/Geographical information</b>	
<b>Land, fylke/Country</b> Norway	<b>Havområde/Offshore area</b>
<b>Kommune/Municipality</b> Stryn	<b>Felt navn/Field name</b>
<b>Sted/Location</b> Grasdalen	<b>Sted/Location</b>
<b>Kartblad/Map</b>	<b>Felt, blokknr./Field, Block No.</b>
<b>UTM-koordinater/UTM-coordinates</b> Zone: East: North:	<b>Koordinater/Coordinates</b> Projection, datum: East: North:

<b>Dokumentkontroll/Document control</b>					
<b>Kvalitetssikring i henhold til/Quality assurance according to NS-EN ISO9001</b>					
<b>Rev/Rev.</b>	<b>Revisjonsgrunnlag/Reason for revision</b>	<b>Egenkontroll av/Self review by:</b>	<b>Sidemanns-kontroll av/Colleague review by:</b>	<b>Uavhengig kontroll av/Independent review by:</b>	<b>Tverrfaglig kontroll av/Interdisciplinary review by:</b>
0	Original document	2022-04-07 Peter Gauer	2022-04-07 Sean Salazar		

<b>Dokument godkjent for utsendelse/ Document approved for release</b>	<b>Dato/Date</b> 7 April 2022	<b>Prosjektleder/Project Manager</b> Christian Jaedicke
--	----------------------------------	--



NGI (Norwegian Geotechnical Institute) is a leading international centre for research and consulting within the geosciences. NGI develops optimum solutions for society and offers expertise on the behaviour of soil, rock and snow and their interaction with the natural and built environment.

NGI works within the following sectors: Offshore energy – Building, Construction and Transportation – Natural Hazards – Environmental Engineering.

NGI is a private foundation with office and laboratories in Oslo, a branch office in Trondheim and daughter companies in Houston, Texas, USA and in Perth, Western Australia

[www.ngi.no](http://www.ngi.no)

NGI (Norges Geotekniske Institutt) er et internasjonalt ledende senter for forskning og rådgivning innen ingeniørrelaterte geofag. Vi tilbyr ekspertise om jord, berg og snø og deres påvirkning på miljøet, konstruksjoner og anlegg, og hvordan jord og berg kan benyttes som byggegrunn og byggemateriale.

Vi arbeider i følgende markeder: Offshore energi – Bygg, anlegg og samferdsel – Naturfare – Miljøteknologi.

NGI er en privat næringsdrivende stiftelse med kontor og laboratorier i Oslo, avdelingskontor i Trondheim og datterselskaper i Houston, Texas, USA og i Perth, Western Australia.

[www.ngi.no](http://www.ngi.no)

Neither the confidentiality nor the integrity of this document can be guaranteed following electronic transmission. The addressee should consider this risk and take full responsibility for use of this document.

This document shall not be used in parts, or for other purposes than the document was prepared for. The document shall not be copied, in parts or in whole, or be given to a third party without the owner's consent. No changes to the document shall be made without consent from NGI.

Ved elektronisk overføring kan ikke konfidensialiteten eller autentisiteten av dette dokumentet garanteres. Adressaten bør vurdere denne risikoen og ta fullt ansvar for bruk av dette dokumentet.

Dokumentet skal ikke benyttes i utdrag eller til andre formål enn det dokumentet omhandler. Dokumentet må ikke reproduseres eller leveres til tredjemann uten eiers samtykke. Dokumentet må ikke endres uten samtykke fra NGI.

